DISEASE SIGNATURE EXTRACTION FOR OBSESSIVE COMPULSIVE
DISORDER USING EFFECTIVE CONNECTIVITY ANALYSIS BASED ON
DYNAMIC CAUSAL MODELLING

A THESIS SUBMITTED TO
THE GRADUATE SCHOOL OF NATURAL AND APPLIED SCIENCES
OF
MIDDLE EAST TECHNICAL UNIVERSITY

BY

ALİCAN YÜKSEL

IN PARTIAL FULFILLMENT OF THE REQUIREMENTS
FOR
THE DEGREE OF MASTER OF SCIENCE
IN
ELECTRICAL AND ELECTRONICS ENGINEERING

FEBRUARY 2016

Approval of the thesis:

DISEASE SIGNATURE EXTRACTION FOR OBSESSIVE COMPULSIVE DISORDER USING EFFECTIVE CONNECTIVITY ANALYSIS BASED ON DYNAMIC CAUSAL MODELLING

submitted by **ALİCAN YÜKSEL** in partial fulfillment of the requirements for the degree of **Master of Science in Electrical and Electronics Engineering Department, Middle East Technical University** by,

Prof. Dr. Gülbin Dural Ünver
Dean, Graduate School of **Natural and Applied Sciences**   _____

Prof. Dr. Gönül Turhan Sayan
Head of Department, **Electrical and Electronics Engineering**   _____

Prof. Dr. Uğur Halıcı
Supervisor, **Electrical and Electronics Eng. Dept., METU**   _____

Prof. Dr. Metehan Çiçek
Co-supervisor, **Faculty of Medicine, Ankara University**   _____

Examining Committee Members:

Prof. Dr. Gözde Bozdağı Akar
Electrical and Electronics Engineering Dept., METU   _____

Prof. Dr. Uğur Halıcı
Electrical and Electronics Engineering Dept., METU   _____

Prof. Dr. Metehan Çiçek
Faculty of Medicine, Ankara University   _____

Prof. Dr. Nevzat Güneri Gencer
Electrical and Electronics Engineering Dept., METU   _____

Assoc. Prof. Dr. İlkay Ulusoy
Electrical and Electronics Engineering Dept., METU   _____

Date: _____

I hereby declare that all information in this document has been obtained and presented in accordance with academic rules and ethical conduct. I also declare that, as required by these rules and conduct, I have fully cited and referenced all material and results that are not original to this work.

Name, Last Name: ALİCAN YÜKSEL

Signature   :

ABSTRACT

DISEASE SIGNATURE EXTRACTION FOR OBSESSIVE COMPULSIVE
DISORDER USING EFFECTIVE CONNECTIVITY ANALYSIS BASED ON
DYNAMIC CAUSAL MODELLING

Yüksel, Alican

M.S., Department of Electrical and Electronics Engineering

Supervisor   : Prof. Dr. Uğur Halıcı

Co-Supervisor   : Prof. Dr. Metehan Çiçek

February 2016, 99 pages

In neuroscience, there exist some studies on activations of human brain used to detect mental disorders and to extract their signatures. Obsessive Compulsive Disorder (OCD) is one of the most common mental disorder that is encountered. Although there are many studies concern about this disorder by using functional Magnetic Resonance Imagining (fMRI), there exist very limited studies for extracting OCD signature that is extracting features from brain activity data to discriminate successfully OCD and healthy subjects. Unlike the past studies which used functional connectivity analysis on fMRI to extract signature of OCD, the aim of this work is to discriminate human brain activities between OCD patients and healthy ones by using effective connectivity analysis. For this purpose, Dynamic Causal Modelling (DCM) is used on the task related fMRI data that were taken from 12 healthy people and 12 OCD patients. Models are estimated by Bayesian Method by fitting the predicted BOLD signals to real signals measured and so to determine the best fitted neuronal state parameters. After that, these effective connectivity parameters are used as features for each subject and Support Vector Machine (SVM) classification method is used to discriminate OCD and control group.

Keywords: Obsessive Compulsive Disorder, Dynamic Causal Modelling, fMRI
Support Vector Machine

ÖZ

NEDENSEL DİNAMİK MODELLEMEYE DAYALI EFEKTİF
BAĞLANTISALLIK ANALİZİ KULLANILARAK OBSESİF KOMPULSİF
BOZUKLUK İÇİN HASTALIK İMZASI ÇIKARILMASI

Yüksel, Alican

Yüksek Lisans, Elektrik ve Elektronik Mühendisliği Bölümü

Tez Yöneticisi   : Prof. Dr. Uğur Halıcı

Ortak Tez Yöneticisi   : Prof. Dr. Metehan Çiçek

Nörobilim alanında, zihinsel hastalıkları tespit etmek ve bu hastalıkların imzasını çıkartmak için insan beynindeki aktivasyonlar üzerine çalışmalar yapılmaktadır. Obsesif Kompulsif Bozukluk (OKB) da çok sık karşılaşılan zihinsel hastalıklardan birisidir. İşlevsel Manyetik Rezonans Görüntüleme (iMRG) tekniği kullanılarak bu hastalık üzerine birçok çalışma yapılmasına rağmen, hastalık imzasının çıkarılması üzerine yapılan çalışmalar çok kısıtlıdır. iMRG ile işlevsel bağlantısallık analizi kullanılan eski çalışmaların aksine, bu çalışmanın amacı efektif bağlantısallık kullanılarak OKB hastaları ile sağlıklı insanların beyin aktiviteleri arasındaki farkı tespit etmektir. Bu amaç doğrultusunda, 12 OKB hastası ve 12 sağlıklı insandan alınmış görev temelli iMRG verileri üzerine Dinamik Nedensel Modelleme (DNM) kullanılmıştır. Modeller öngörülen ve ölçülen işaretleri eşleyen Bayesçi method kullanılarak tahmin edilmiştir. Bu method aynı zamanda en uyumlu efektif bağlantısallık değerlerini de belirlemiştir. Bu aşamadan sonra, bulunan efektif bağlantısallık değerleri her bir kişi için özellik olarak kullanılmıştır ve bu özellikler ile OKB hastaları ve sağlıklı kişiler Destek Vektör Makinesi (DVM) ile sınıflandırılımıştır.

Anahtar Kelimeler: Obsesif Kompulsif Bozukluk, Dinamik Nedensel Modelleme
iMRG, Destek Vektör Makinesi

to my wife...

ACKNOWLEDGMENTS

TABLE OF CONTENTS

LIST OF TABLES

LIST OF FIGURES

FIGURES

LIST OF ABBREVIATIONS

AU-BAUM	Ankara Universitesi Beyin Araştırma ve Uygulama Merkezi
BSM	Bayesian Model Selection
BOLD	Blood Oxygen Level Dependent
DCM	Dynamic Causal Modelling
dHb	De-oxygenated hemoglobin
DTI	Diffusion tensor Imaging
EEG	Electroencephalogram
FFX	Fixed Effects
fMRI	Functional Magnetic Resonance Imaging
GMM	Gaussian Mixture Model
Hb	Hemoglobin
HDR	Hemodynamic Response
IC	Insular Cortex
IPL	Inferior Parietal Lobe
LOOCV	Leave One Out Cross Validation
MEG	Magnetoencephalogram
MNI	Montreal Neurological Institute
MRI	Magnetic Resonance Imaging
OCD	Obsessive-Compulsive Disorder
PCC	Posterior Cingulate Cortex
PPI	Psycho-physiological Interactions
rCBF	Regional Cerebral Blood Flow
RFX	Random Effects
SEM	Structural Equation Modelling
SFP	Superior Frontal Gyrus
SVM	Support Vector Machine
VAR	Vector Autoregressive
VOI	Volume of Interest

CHAPTER 1

INTRODUCTION

In neuroscience, there are many studies on mental diseases and the characteristic features and the abnormalities of them have been examined for last decade. Obsessive Compulsive Disorder (OCD) is one of the psychological disorder that is characterized "by the presence of repetitive invasive impulses called obsessions which cause recurrent behaviours named compulsions" [8][9].

Functional Magnetic Resonance Imaging (fMRI) is one of the best MR technique to understand how human brain works during a given task or in resting state. In recent years, fMRI is used in many studies to detect functional abnormalities among regions of brain [4] and pattern recognition methods are applied on fMRI data to discriminate subjects with mental disorder from healthy subjects. Disease Signature (biomarker) extraction aims to find a set of features that can be used successfully to discriminate subjects having the related disorder.

Although there are some disease signature studies related to other disorders, the studies related to OCD are quite limited. In a very recent survey related to application of pattern recognition approaches for detection of mental disorders [5], several studies related to mental disorders are listed. In this survey, only four studies related to OCD are mentioned [8][10][11][12]. The Table 1.1 adapted from this survey shows the current status of pattern recognition studies related to OCD.

In [11], structural MRI data is used. For classification, they do not apply any machine learning algorithm but they decide on the subject class by calculating the euclidean distances between individual participants and the mean of OCD and control group

based on structural MRI data. Their results are that OCD people are distinguished from healthy control group with 93.1% accuracy when they applied cross validation among existing subjects. This result was very promising for signature study. However, the authors examined anatomy of the brain without a stimuli. Since behaviours of OCD and healthy group under a given task is examined in this thesis work, their dataset is not applicable. Lastly, their independent test results has 76.6% accuracy for classification of new subject.

In [8], researchers use different methods to analyse OCD fMRI data. There were two tasks in their study: fear and disgust. The pictures that they showed to the subjects include fear, disgust and neutral objects. At first, they determine *the volumes* in fMRI where the activation was occurred when fear and disgust pictures were shown. In order to determine these volumes, they used *discriminating volumes* method introduced in [10]. After this step, Weygant and his co-workers use *searchlight* method which compares clusters which have three-voxel size radius inside the discriminating volume for each task. Their study was conducted with 10 OCD and 10 control groups and they claim that, they reached 100% discrimination between OCD and healthy groups when fear-inducing pictures were shown. However they have reached this accuracy only at three points (MNI: (6, 56, -10) ; (6, 62, -10) and (-14, 18, 2)) so their results show that these areas are significantly activated when fear related task is used.

It is mentioned in the survey [1] that Li et al.,[12] have used Diffusion Tensor Imaging (DTI) for 28 OCD and 28 control people. DTI is simply magnetic resonance imaging method allowing the mapping of the diffusion process of water molecules and it is mainly used for structural analysis. The authors have obtained 84% accuracy with SVM classifier.

Among these studies mentioned in Table 1.1, the study [10] was conducted at Middle East Technical University (METU) jointly with Ankara University Brain Research Center (AU-BAUM). This study originally considered the resting state fMRI data for OCD [11] and functional connectivity analysis was used to extract features. The study was later extended to cover task related fMRI data [10] under imagination task described in [2]. In fact, the data used in these OCD disease signature studies given in [10] and [13] were collected in the previous study [2] conducted at AU-BAUM,

which is going to be used also in this thesis work. In this dataset, there were two main tasks which are *suppression* and *erasing* and there were three other tasks, which are *imagining* task used to trigger experiment, *free imagining* task used to get neutral state; and *resting* state used between main tasks and neutral task. The data were collected for subjects which consist of 12 OCD patients and 12 control group people.

The recognition performance for OCD Signature based on functional connectivity obtained from resting state fMRI [13] was 69% (when SVM applied on similarity is used) and it is increased to 74% when the task related fMRI were used instead of resting state, while keeping the feature extraction and classification steps the same. This is the motivation behind this thesis study to further examine task related fMRI data for OCD signature extraction.

However, in order to analyse task-related responses of brain activities, effective connectivity should also be concerned beside functional connectivity. Since the confounding effects of stimulus-evoked responses interact other brain regions, this interaction may overcome input effects. However, effective connectivity discards these influences because "one neuronal system exerts on another in that connectivity analysis" [14]. Therefore, the aim of this study is to examine the differentiability of brain activities between OCD patients and a control group by using effective connectivity analysis.

In this thesis study, a novel OCD signature extraction method based on effective connectivity analysis using Dynamic Causal Model (DCM) is proposed. The steps of the proposed method is briefly as follows. At the first step, the raw fMRI data undergo preprocessing step with SPM8 software (Wellcome Department of Cognitive Neurology, London, UK) in MATLAB (Math works, Sherborn, Mass., USA) to reduce noises and discriminate confounds due to head movement etc. Afterwards, Volume of Interest (VOI) Extraction is applied to these preprocessed data to create fMRI time series from activated regions. These time series are used for Dynamic Causal Modelling (DCM) analysis. In DCM, activated regions and defined connections between them form a neuronal network which is the base of the DCM analysis. This network also reduces the complexity and increases the affect of analysis. This work grounds on the results in [2] and the neuronal network has been established with the help of

3

this study. There are many state parameters to be optimised in DCM analysis and with the help of Estimation-Maximization algorithm, their optimized values are found and the best suited model is chosen with Bayesian model selection.

Pattern recognition is used to classify a new examplar (pattern) by using information constructed by previous patterns. In literature, pattern recognition is used in many areas such as signal and image processing, medicine, computer vision etc. Also, in neuroscience, pattern recognition has received much attention. Craddoeck et al., [15] in order to estimate the disease state from rsFC data, they used pattern recognition. Also, Shen et al., [16] use again pattern recognition to detect schizophrenia disease. Finally, Manuel and Ao [17] use different pattern recognition algorithm to classify two different type of classes fMRI data. In this study, after obtaining the best neuronal model by applying DCM analysis, their connectivity parameters which represent the amount of effective connectivity are used as features to classify healthy and OCD groups. Support Vector Machine (SVM) is used in this study since it is widely applied in fMRI studies successfully [10][13][18].

The rest of this thesis is organized as follows: In Chapter II, background information on fMRI, DCM and the classification method SVM is provided. Afterwards, in Chapter III, the data set used and the method proposed are explained in detail. In chapter IV, OCD signature for the data is proposed together with the classification method. In chapter V, results of the study and some discussions are given. Finally, in chapter VI, the study is concluded.

Table 1.1: Pattern recognition studies related to classification of Obsessive compulsive Disorder (OCD) versus Control group, LOO-CV stands for Leave One Out cross Validation[1]

Authors, Year	Sample Size	Age Group	Modalities	Features	Classifiers	Validation	Classification Performance (Accuracy)
Soriano-Mas et al.,2007[11]	OCD=72 Cont.=72 Rep. OCD=30 Cont.=30	Adults	Structural MRI	Neither feature set, mean difference value of OCD and controls	N.S.	Test Validation	76.60%
Weygandt et al.,2012a[8]	OCD=10 Cont.=10	Adults	Task fMRI-Emotional Images	Voxel based feature set and automatic feature selection	SVM	LOO-CV	100.00%
Shenas et al.,2014[10]	OCD=12 Cont.=12	Adults	rs-fMRI - Task fMRI-Imagination	Region based feature set and automatic feature selection	LDC; SVM	LOO-CV	74.00%
Li et al.,2014[12]	OCD=28 Cont.=28	Adults	Diffusion MRI	Voxel based feature set	SVM	LOO-CV	84.50%

CHAPTER 2

THEORETICAL BACKGROUND

2.1 Functional Magnetic Resonance Imaging

Functional Magnetic Resonance Imaging (fMRI) is the most common technique to measure brain activity. As its name implies, fMRI is a neuroimaging technique that uses standard MRI scanners to investigate changes in brain function over time. Standard MRI uses strong magnetic fields and radio waves delivered at resonance frequency. Imaging part is to gather responses of materials in scanned areas to the applied magnetic energy.

The difference of fMRI from standard scanning techniques is what it measures. fMRI is used to scan not only structural image like classical MRI do but also functional activities on the scanned area. Since functional activities are issued, the brain activities is the main concern of fMRI technique.

The development of fMRI is based on the remarkable discovery on magnetic property of hemoglobin molecule by Pauling and Coryell in 1936 [19]. This milestone was based on the hemoglobin molecule, which carries oxygen in vascular systems, have different magnetic property if it bounds the oxygen. It should be noted that since diamagnetic materials have no unpaired electrons and zero magnetic moment, they have the property of a weak repulsion from a magnetic field. Therefore, under magnetic fields, diamagnetic materials do not disturb MR signals. When hemoglobin molecules are not bounded to the oxygen (de-oxygenated hemoglobin, dHB), they behave like paramagnetic materials but if they are bounded to the oxygen (oxygenated hemoglobin, Hb) they become diamagnetic materials. However, the discovery of

fMRI was devoted to Seiji Ogawa et al. [3]. They investigated the possibility of examining brain physiology using MRI by proposing Blood Oxygen Level Dependent (BOLD) contrast which depended on the discovery of magnetic properties of hemoglobin. Figure 2.1 shows the results of experiment conducted by Ogawa and his team. It was shown that oxygenated blood was perfectly scanned while deoxygenated blood had distortions.

A   B
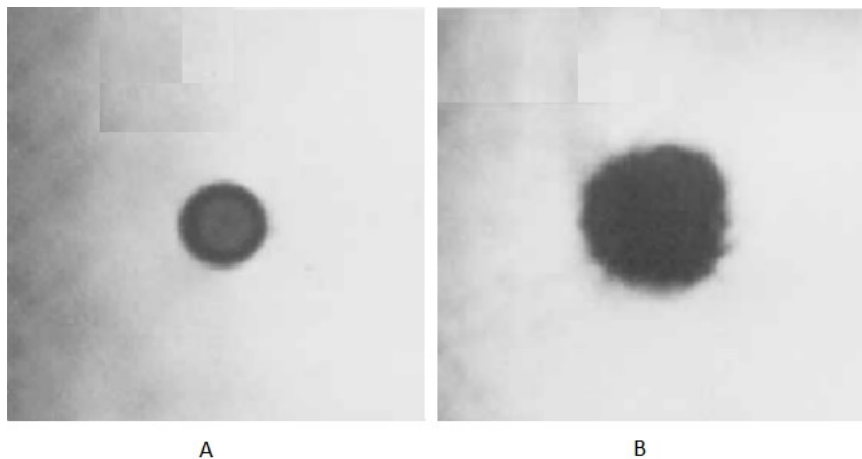
Figure 2.1: The images of (A) oxygenated and (B) dexoygenated blood [3]

BOLD contrast imaging is the base of the fMRI. It scans with oxygenated blood very well and takes into consideration the relation between functional activities and oxygen level in blood. With very basic biological inference that if one area is activated, then the amount of oxygen in there is decreased due to energy consumption. Therefore, there seems to be in an opposite way to detect activation on a specific area because the existent of oxygen (oxygen is bounded hemoglobin) supports the MR signals. However, the biological response expresses this conflict that when one area has an activation, first deoxygenated blood level is increased, then due to biological responses of the body, oxygenated blood level is increased on that area. BOLD contrast imaging captures this contrast to determine activated areas of brain.

This biological response can be associated with the hemodynamic response (HDR) which is defined as the change in MR signal triggered by the neuronal activity.

After the discovery of that BOLD contrast is highly correlated with activations, fMRI technique became popular in neuroscience studies. Although other imagining tech-

niques like EEG and MEG have their own advantages and still be used, fMRI is preferred widely due to its functional response as well as temporal and spatial resolutions. In Figure 2.2, activations detected by fMRI technique are shown.
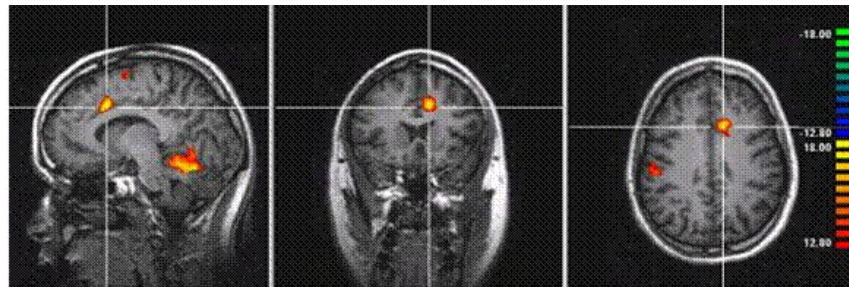
Figure 2.2: fMRI Images show "Training Effect in Rostral Anterior Cingulate Cortex",[4]

Since fMRI has an ability to observe activations on the brain, there have been many studies published with fMRI [20][21]. Also, the neuroscientists use this technique as a background for studies in many areas: discriminate brain states due to different tasks applied to subject [17], define brain network at resting state [22] or determine features of mental disorders such as Alzheimer, Schizophrenia, OCD [23][10].

2.2 Effective Connectivity Analysis

In neuroscience, the connectivity analysis with fMRI is a hot topic. For connectivity analysis on brain, the neuroscientists have suggested three models: (i) anatomical or structural connectivity, (ii) functional connectivity and (iii) effective connectivity. By using these connectivity analyses, the neuroscientist try to find relationships among brain regions when an activation is occurred. Structural connectivity is examined how physical connections among brain regions effect behaviours or activations [8]. On the other hand, functional connectivity is used to find statistical dependencies between regional time series from active regions of the brain and there are many studies on functional connectivity analysis on fMRI. Lastly, effective connectivity, also used in this thesis study, examines the directed influences between neurons or neuronal populations[14].

Effective connectivity deals with interactions among regions when activation is oc-

curred due to input or stimuli tasks. The neuronal state of the brain changes with an applied input or stimuli because the brain regions show some reactions against to these inputs. Reasons of these responses are the relationships between regions and effects of input on that regions or effect of state changes itself. These parameters on effective connectivity are characterised and analysed in this study.

In literature there are various models of effective connectivity such as Psycho-physiological Interactions (PPI), Structural Equation Modelling (SEM) and Vector Autoregressive (VAR) or Dyanmic Causal Modelling (DCM)[24][25]. While the classical model PPI, SEM or VAR operate on measured level, DCM uses a dynamic model approach defined on neuronal states and takes causality into consideration [24]. The interactions between brain regions on neuronal states depend on subject and biological structure of his brain. Therefore, in order to analyse this connectivity, there should be a dynamic system model representing these states and their connectivities. Dynamic Causal Modelling (DCM), proposed in [24] is a special case of the Dynamic System Model and it is used in order to find effective connectivity among brain regions represented by state variables.

2.2.1 Dynamic Causal Modelling

There are some techniques of effective connectivity like PPI, SEM or VAR. These methods work at measured level. This is a problem to determine causal system because "it is located at neuronal level which cannot be investigated directly using these methods" [25]. In order to overcome this problem, models that combine two things are required: "...a parsimonious but neurobiologically plausible model of neural population dynamics, and a biophysically plausible forward model that describes the transformation from neural activity to the mesaured signal" [26]. In DCM, these two models are called as **neuronal network** and **hemodynamic response** respectively. These models allow to fit together the parameters of the hidden neuronal state and forward model such that the predicted time series are optimally similar to the observed time series. DCM is the only approach combining models of neural dynamics and biophysical forward models. [25].

DCM was introduced in 2003 for fMRI data [24], the equations and applications

of DCM for fMRI have since been refined and extended repeatedly [27][28][29]. DCM are generative models of brain responses, which provide posterior estimates of neurobiologically interpretable quantities. DCM are defined by four features:

1) DCM is dynamic. It uses differential equations for describing hidden state (neuronal dynamics).

2) It has causality due to describing how dynamics in one neuronal population cause dynamics in another and how these interactions are modulated by experimental manipulations or endogenous brain activity.

3) DCM uses a biophysically motivated and parametrized forward model to link the modelled neuronal dynamics to specific features of measured data.

4) DCM uses Bayesian Model Selection[30].

DCM analysis simply, uses the established hidden neuronal circuit and convolves this circuit with hemodynamic response in order to generate predicted BOLD signals. These predicted signals are compared with real BOLD signals and with expectation-maximization, these two signals are tried to be fitted by arranging neuronal circuit parameters so that the best neuronal circuit is established.

DCM analysis includes many parameters and much attention should be taken when one concerns with it. These considerations were summarized in [30]. At first, model space should be defined carefully. The brain has an enormous number of connections and neurons and there may be extremely large number of model. In order to analyse a special task, one should know which regions are activated. Therefore, model space should be established so that neuronal network structures or network parameters are useful. Secondly, beside log evidence and group Bayes factor (GBF), random effect analysis was proposed in [41] for group analysis to compare possible models.

In literature, there are many studies on DCM concerned in cognitive neuroscience, including memory [31], learning [32] and language [33]. There are also many studies concerning mental disorders [34]. All these works use common flowchart to use DCM. This flow was established in [30].

In order to estimate neuronal state and hemodynamic response parameters, DCM uses

a Bayesian approach. According to this approach there are two steps that should be applied.

1. It must be specified the likelihood function which requires the assumption about the noise.

2. It must be specified the prior parameters which are interested.

In order to implement these two steps, DCM uses principle nature priors like Blood volume deoxyhemoglobin content.

The flowchart given in Figure 2.3 represents the Hemodynamic forward model and it includes three main parts.
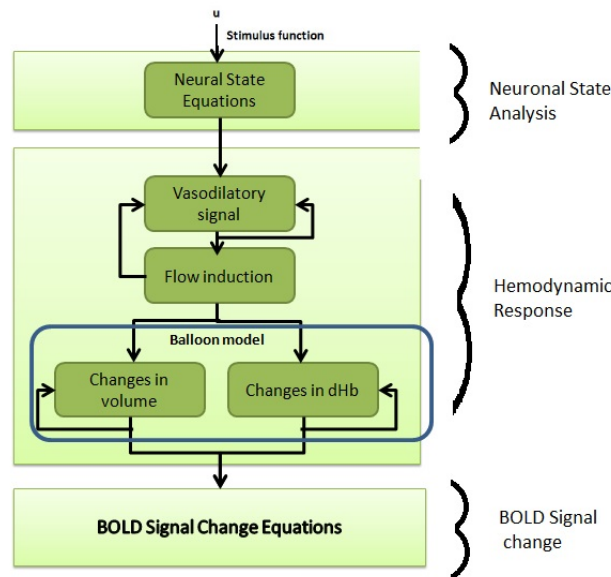
Figure 2.3: Hemodynamic Forward Model [5]

1. In the first part, the challenge is to find the linkage between neural activity and regional cerebral blood flow (rCBF). The neural state equations describe the dynamic behaviours of the underlying neuronal circuit in response to the applied stimulus.

2. The second part is called as Hemodynamic response equations and it includes Ballon Model which examines the dependency of BOLD signal on the blood volume and deoxyhemoglobin content. This part represent the biological effect of DCM analysis.

3. The third part is the output of the model and it represents BOLD signal change

equations

These parts of DCM are explained in detail in the following sections.

2.2.1.1   Neuronal State Analysis

Activations on neuronal states cannot be measured directly with fMRI however effective connectivity helps to understand these states by structural or functional MRI scanner techniques. In DCM analysis, firstly a neuronal circuit is established among some regions to represent effective connectivity effected by inputs or stimulations. The dynamic of this neuronal circuit is described through effects of neuronal states and input representing stimulus.

In [24], the neuronal state changes as defined in Equation 2.1

$$\frac{dz}{dt} = F(z, u, \theta)$$
$$\theta = (A, B, C)$$

(2.1)

where $\frac{dz}{dt}$ represents state changes, z is present state, u is input and θ is internal parameters of the circuits. θ consist of three neuronal parameters representing the connection strengths among the neuronal circuit elements, i.e. they are the effective connectivity parameters. The first one, called A parameter in this work, describes the intrinsic connections between nodes. This parameter is very important for effective connectivity because it represents the affect of one region on another. The second parameter is B parameter and it represents modulatory effects of stimulations on connections and the last one is the C parameter which shows the direct affect of input on the regions.

The neuronal state can be expressed in terms of state parameters as given in Equation 2.2

(2.2)

$$\dot{x} = \left(A + \sum_{j=1}^{m} u_j B^{(j)} \right) x + Cu$$

13

Therefore, in DCM, the neuronal state can be shown in Equation 2.3

$$F(x, u, \theta) = \left(A + \sum_{j=1}^{m} u_j B^{(j)} \right) x + Cu$$

$$A = \frac{\delta F}{\delta x}|u = 0$$

$$B^{(i)} = \frac{\delta^2 F}{\delta x \delta u_i} = 0 \qquad (2.4)$$

$$C = \frac{\delta F}{\delta u}|x = 0$$

When the parameter $B = 0$, then the system becomes linear. In this thesis linear case will be considered.

In Figure 2.4, a sample of linear neuronal circuit and its connections are shown.
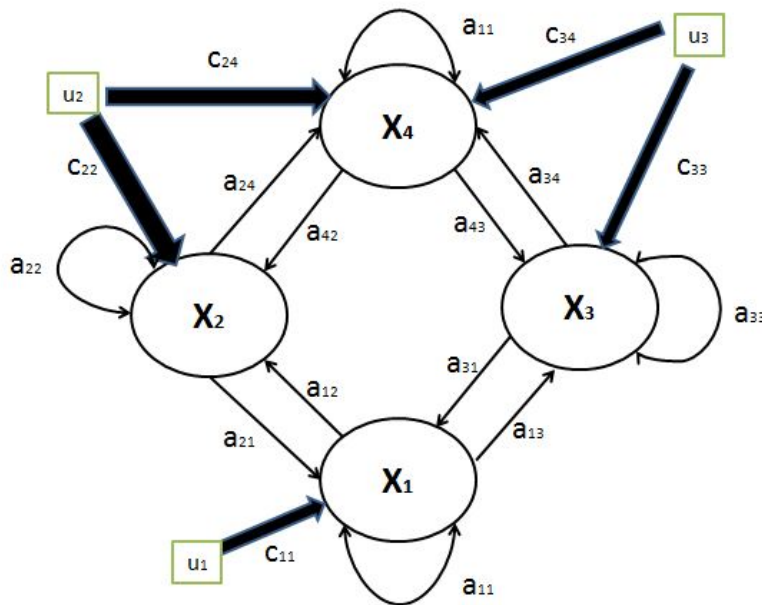
Figure 2.4: Representation a sample neuronal state [6]

The matrix form of this representation is as shown in Equation 2.5

14

$$
\begin{bmatrix} \dot{x}_1 \\ \dot{x}_2 \\ \dot{x}_3 \\ \dot{x}_4 \end{bmatrix} = \begin{bmatrix} a_{11} & a_{12} & a_{13} & 0 \\ a_{21} & a_{22} & 0 & a_{24} \\ a_{31} & 0 & a_{33} & a_{34} \\ 0 & a_{42} & a_{43} & a_{44} \end{bmatrix} \begin{bmatrix} x_1 \\ x_2 \\ x_3 \\ x_4 \end{bmatrix} + \begin{bmatrix} c_{11} & 0 & 0 \\ 0 & c_{22} & 0 \\ 0 & 0 & c_{33} \\ 0 & c_{24} & c_{34} \end{bmatrix} \begin{bmatrix} u_1 \\ u_2 \\ u_3 \end{bmatrix} \tag{2.5}
$$

2.2.1.2 Hemodynamic Response

According to the DCM, there should be a transfer function to map hidden neuronal circuit parameter to the observable output level. Hemodynamic response, which differs DCM from other effective connectivity models, was proposed in [35]. Hemodynamic response represents the effects of anatomical parameters for the calculation of the output signal. There should also be equations to represent hemodynamic response for DCM analysis. It has been very compelling calculation until David et. al., showed that the hemodyanamic model is a necessity for effective connectivity.

Hemodynamic response model as seen in Figure 2.3 , consists of two parts. The Balloon model and Neurovascular state.

The Balloon Model   The Balloon model is proposed by Buxton and Frank, in order to represent two important factor to create BOLD signals: blood volume (v) and deoxyhemoglobin content (q) and there are two assumptions for these parameters [36]

1. The reaction of small past-capillary vessels to the increase of inflowing blood is like an inflating blood

2. The extraction of oxygen is tightly related to the blood flow

The first assumption states that the changes in blood volume (v) correspond to differences in inflow and outflow of blood within a time constant and the second assumption states that the change in the deoxyhemoglobin content (q) correspond to the difference of delivery of deoxyhemoglobin into the venous components between the expulsion of deoxyhemoglobin from the venous components. Therefore, from these inferences there are two differential equations for blood volume in Equation 2.6

and deoxyhemoglobin content in Equation 2.7

$$\tau\frac{\delta v(t)}{\delta t} = f(t) - v(t)^{\frac{1}{\sigma}} \tag{2.6}$$

where τ is the mean transit time in blood, f(t) flow of blood within a time constant and v(t) is the blood volume at t and σ is the resistance of venous balloon

$$\tau\frac{\delta q}{\delta t} = f(t)\frac{1 - (1 - E_0)^{\frac{1}{f}}}{E_0} - v(t)^{\frac{1}{\sigma}}\frac{q(t)}{v(t)} \tag{2.7}$$

where E_0 initial oxygen extraction fraction and q(t) deoxyhemoglobin content at t, τ is the mean transit time in blood, f(t) flow of blood within a time constant and v(t) blood volume at t and σ is the resistance of venous balloon

The detail of the calculations of these equations can be found at [36]

Neurovascular State The vascular response also effects the output BOLD signals. Friston et. al.,[37], developed a model for vascular responses in Equation 2.8

$$\frac{\delta s(t)}{\delta t} = x - \kappa s - \gamma(f - 1) \tag{2.8}$$

where κ is the rate constant of signal decay, γ is the rate constant feedback regulations, f(t) is the normalized flow and s=$\frac{df(t)}{dt}$

2.2.1.3 BOLD Signal Change Equations

Real MRI signal is represented by the change in BOLD Signal. With the help of Hemodynamic Forward Model, BOLD Signal Change can be calculated in effective connectivity analysis. These results are tried to be optimised with the measured BOLD signal change and thus effective connectivity parameters can be calculated. The calculated BOLD signal change equations were given in [38] as in Equation 2.9.

16

$$\lambda(q, v) = \frac{\Delta S}{S_0} \approx V_0 \lfloor k_1(1 - q) + k_2(1 - \frac{q}{v}) + k_3(1 - v) \rfloor$$

$$k_1 = 4.3\vartheta_0 E_0 TE$$

$$k_2 = \epsilon r_0 E_0 TE \tag{2.9}$$

$$k_3 = 1 - \epsilon$$

2.2.1.4 Bayesian Method For Model selection

Dynamic Causal Modelling (DCM) analysis is used to find the best explanations of effective connectivity on hidden neuronal states. It predicts possible BOLD signals from this network and compares with the real output. After creating hemodynamic forward model with unknown parameters between neural state and observation level, the model best fitting the data should be selected. Therefore, a method to fit these two output and to estimate parameters of the hidden state equations is needed. In DCM analysis, parameters are estimated by Bayesian method based on Expectation Maximization (EM). Bayes theory says that:

$$p(w|D) = \frac{p(D|w)p(w)}{p(D)} \tag{2.10}$$

where w are the parameters to be adjusted, $p(w)$ is called as the *prior probability* since it depends on assumptions before observing the data D. After D is observed, $p(w|D)$ becomes *posterior probability*. $p(D|w)$ is evaluated for the observed data set D and can be viewed as a function of the parameter vector w, called *likelihood function*. Therefore, Bayes method is simply

$$posterior \propto likelihood \mathrm{x} prior \tag{2.11}$$

In model selection approach, Bayes' theorem can be expressed as

$$p(m_i|y) \propto p(m_i)p(y|m_i) \tag{2.12}$$

where m_i represents a set of models, i=1,...,N and y is the observed data. The prior distribution is $p(m_i)$ which estimates how likely the model. For model selection, since there is no assumption before the observation, the prior distributions are assumed to be equal to each other. The term $p(y|m_i)$ is the model evidence which represents the choice by the observed data y for different models. It is also called as *marginal likelihood* since it is the likelihood function over the space of model. In summary, the evidence model simply finds the situation which maximizes the probability of output data y when a model m is given, i.e. maximizes the *posterior probabity*. It also concerns with θ which reflects the parameters of neuronal state, i.e. $\theta(A, C)$, Equation 2.13 expresses evidence model based on the Bayesian method

$$
\begin{aligned}
p(y|m) &= \int p(y, \theta|m)d\theta \\
&= \int p(y|\theta, m)p(\theta|m)d\theta
\end{aligned}
\tag{2.13}
$$

Since there are many possible models for DCM analysis, probabilities of models, even for the best model, are generally a small number, thus *log-evidence model* is used because log value of the small numbers may be large. This form is the log value of model evidence selection. The log evidence is defined as in Equation 2.15

$$
\begin{aligned}
logp(y|m) &= accuracy(m) - complexity(m) \\
&= logp(y|\theta, m) - complexity(m)
\end{aligned}
\tag{2.14}
$$

where $logp(y|\theta, m)$ is the log likelihood function.

The log evidence for a model m consists of two terms which are accuracy and complexity. When complexity of the model is low, then the accuracy of the model should be high. On the other hand, when complexity is increased, the relative accuracy is decreased. For the accuracy term, *log likelihood* function of the model m is used and for the complexity, there are three known approximation methods.

1. Akaike Information Criterion (AIC)

2. Bayesian Information Criterion (BIC)

3. Negative Free Energy (F)

$$\text{AIC} = log\,p(y|\theta, m) - p \quad \text{where p is the number of parameters}$$
$$\text{BIC} = log\,p(y|\theta, m) - \frac{p}{2}logN \quad \text{where N is the number of data points}$$

<div align="right">(2.15)</div>

Although AIC and BIC methods were used in previous studies, these methods have disadvantages. These methods only take the number of parameters into account and they were found to be not suitable for the dynamics of these parameters. For this reason, a *negative free energy* approximation was proposed in literature. In this model, accuracy term and the expected log likelihood under some posterior are used. KL term after Kullback-Leibler [43] is used for complexity. KL measures the distance between prior and posterior distribution. Final Equation for log likelihood is given below:

$$
\begin{aligned}
p(y|m) \quad &=< log(p(y|\theta, m) > -KL[q(\theta), p(\theta|m)] + KL[q(\theta), p(\theta|y, m)] \\
&= F + KL[q(\theta), p(\theta|y, m)]
\end{aligned}
$$

<div align="right">(2.16)</div>

where F is expressed as the difference between accuracy and complexity

$$F =< log(p(y|\theta, m) > -KL[q(\theta), p(\theta|m)]$$

<div align="right">(2.17)</div>

The main advantage of negative free energy on the other methods is that it has components that express how many parameters are inadequate.

Log evidence can be used for comparison in the model selection. After log evidence is calculated, Bayes Factor can be used to compare models as given in Equation 2.18

$$B_{12} = \frac{p(y|m_1)}{p(y|m_2)}$$

<div align="right">(2.18)</div>

this factor refined by taking equal prior probability for the models, that is $p(m = i)$ and $p(m = j)$

$$p(m = i|y) = \frac{p(y|m = i)}{p(y|m = i) + p(y|m = j)}$$

$$= \frac{1}{1 + \frac{p(y|m=j)}{p(y|m=i)}}$$

$$= \frac{1}{1 + B_{ji}} \tag{2.19}$$

$$= \frac{1}{1 + exp(-logB|ji)}$$

Hence

$$p(m = i|y) = \sigma(logB|ji) \tag{2.20}$$

where the σ is the sigmoud function.

Bayesian factor is also used for group analysis. For this analysis, it is defined as Group Bayes Factor for N subjects [38] (GBF) as

$$GBF_{i,j} = \prod_{n=1}^{N} BF_{i,j}^{(n)} \tag{2.21}$$

Equation 2.21 implies the *fixed effect* analysis based on multiplying the marginal likelihoods over all subjects to build the probability of the group subject data [38] However, fixed effect analysis use the one model posterior probability for one subject.

The other analysis method is called as *random effects* analysis. In this analysis, all models are taken as random variable for the all subjects in the group. There two probabilities defined in this analysis: The *expected probability* is that a given subject have generated data according to a given model and the *exceedance probability* represents the existence that one model is more likely than any other model. Therefore, these probabilities depend on the models interested.

2.3 Pattern Recognition

Pattern recognition has two steps: 1) feature extraction and 2) classification. In this thesis work, the proposed methods are going to use DCM parameters as features. Also, the Support Vector Machine (SVM) method used in the classification. In the following, feature extraction and classification steps are explained. Furthermore, it is described how to measure the performance.

2.3.1 Feature Extraction

Feature extraction is used to form non-redundant and informative variables for each observations and they are used for classification purpose. Features should represent the observations completely in lower dimensions therefore this is sometimes called as dimension reduction methods. In fMRI studies, feature extraction methods were used to increase correlation between neuronal activities and eliminate non redundant information[39].

In [40], the covariance selection (CS) was used as feature extraction method by modelling the correlations between active voxels. Also in [13] ,similarity measurement methods like dot product and cross product and dimension reduction methods Principal Component Analysis (PCA) and Linear Discriminating Analysis (LDA) were used as feature selection methods for fMRI data. In [41], the connectivity parameters were directly used to measure reliability of scan-rescan of percent signal change (PSC) and DCM analysis.

In DCM analysis, expectation-maximisation is used as Bayesian method to estimate connectivity parameters and thus these parameters can be used as features. Since these connectivity parameters are extracted according to measured BOLD time series with neuronal state equations, they are pretended as the task features of each subjects. In this thesis, it is proposed to use the connectivity parameters as features and it is shown that they are powerful in classification of OCD and healthy groups.

2.3.2 Support Vector Machine

Support Vector Machine (SVM) is a widely used statistical pattern recognition classifier and it is based on Vapnik statistical learning theory [42]. SVM simply propose best hyper surface between the classes to separate them from each other. The best hyper surface for an SVM is chosen so that the maximum distance between the feature vectors of different classes know as *margin* is reached. The closest feature vectors of both classes to separating hyper surface are called as *support vectors*. The Figure 2.5 shows the hyperplane boundary, support vectors and examplars where blue and red indicate two different class type.

$\mathbf{w}^T\mathbf{x} + b = 1$

$\mathbf{w}^T\mathbf{x} + b = 0$

$\mathbf{w}^T\mathbf{x} + b = -1$

Support Vector

Support Vector

$\mathbf{w}$
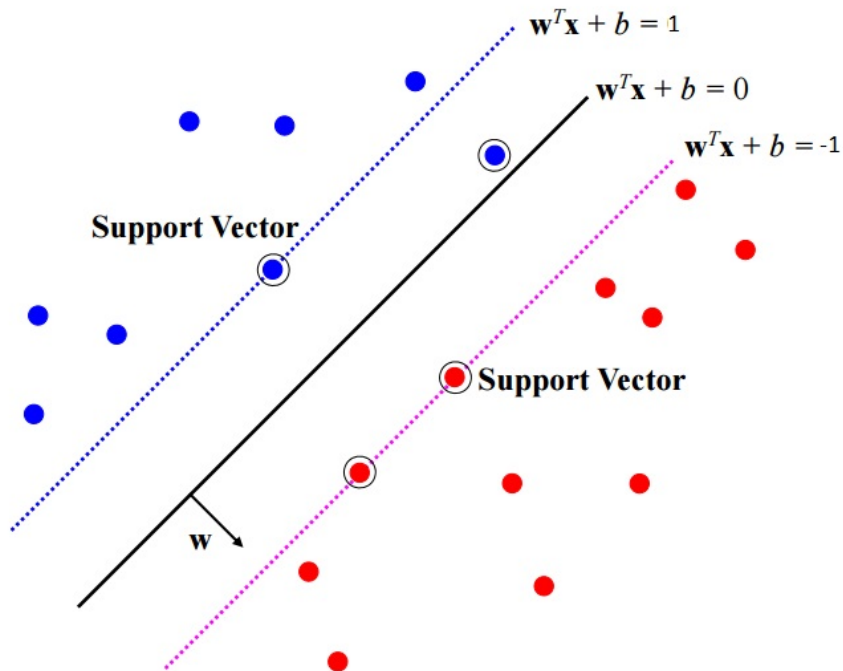
Figure 2.5: Support Vector Machine: hyperplane boundary and support vectors

In support vector machine algorithm, $n-$dimensional data vectors are separated by $(n-1)$ dimensional hyperplane. This separation is called *linear classifier*. There may be many hyperplanes that might classify the data and the best hyperplane is chosen so that it represents the largest separation, or margin, between the two classes. Therefore, the best hyperplane has the maximum distance between support vectors of both classes. If such a hyperplane exists, it is known as the *maximum-margin hyperplane*

and the linear classifier it defines is known as a maximum *margin classifier*[43].

SVM is widely used in fMRI data analysis to separate healthy people and patients using connectivity differences of their brains[44][45][46]. In recent studies, SVM is used for classification of OCD patients[10][13].

Linear SVM Algorithm: Assume a linearly separable k samples of n dimensional training data vector D such that

$$D = \{(x_i, y_i)|x_i \epsilon \mathcal{R}^p, y_i \epsilon \{-1, 1\} \quad i = 1, 2..., n\}$$ (2.22)

where the y_i indicates the class of the point x_i and it is either $+1$ or -1. Each x_i is a $n-$dimensional real valued vector. In SVM, it is tried to find the maximum-margin hyperplane that divides the points having $y_i = 1$ from those having $y_i = -1$. Any hyperplane can be written as the set of points x as long as to satisfy Equation 2.23

$$w \cdot x - b = 0$$ (2.23)

where **w** is the normal vector to the hyperplane and " $\cdot$ " represents the inner dot product. The value $\frac{b}{\|\mathbf{w}\|}$ determines the offset of the hyperplane from the origin along the normal vector **w**.

If the training data are *linearly separable*, two hyperplanes can be chosen in a way that they separate the data and there are no points between them and then try to maximize their distance. These hyperplanes are described by the Equation 2.24

$$\mathbf{w} \cdot \mathbf{x} - b = 1$$
$$\mathbf{w} \cdot \mathbf{x} - b = -1$$ (2.24)

Geometrically, the distance between these two hyperplanes is $\frac{2}{\|\mathbf{w}\|}$, thus in order to maximize the distance between the planes, $\|\mathbf{w}\|$ should be minimized. Also in order

to prevent data points being on the margin slab, the class boundaries are defined as in Equation 2.25 for each i either first or the second condition holds

$$\mathbf{w} \cdot x_i - b \geq 1$$
$$\mathbf{w} \cdot x_i - b \leq -1$$

(2.25)

This can be rewritten as:

$$y_i(\mathbf{w} \cdot x_i - b) \geq 1 \quad \text{for all } 1 \leq i \leq n$$

(2.26)

Therefore, the optimization problem should be concerned as minimize $\|\mathbf{w}\|$ subject to (for any $i = 1, ..., n$) $y_i(\mathbf{w} \cdot x_i - b) \geq 1$

Primal form In order to reduce complexity of the optimization problem, $\frac{1}{2}\|\mathbf{w}\|^2$ (the factor $\frac{1}{2}$ being used for mathematical convenience) is used instead of $\|\mathbf{w}\|$, the norm of $\mathbf{w}$, because it involves a square root. The use of former term does not change the solution and this usage is called as *quadratic programming optimization* problem. More clearly:

$$argmin_{(\mathbf{w},b)} \frac{1}{2}\|\mathbf{w}\|^2$$

(2.27)

subject to

$$y_i(\mathbf{w} \cdot x_i - b) \geq 1 \quad , \text{i=1,...,n}$$

(2.28)

The constraints can be combined to the cost function (in optimization it is called as lost function) by introducing Karush-Kuhn-Tucker (KKT) multipliers α and the previous constrained problem can be expressed as

$$argmin_{(\mathbf{w},b)} max_{\alpha \geq 0}\left\{\frac{1}{2}\|\mathbf{w}\|^2 - \sum_{i=1}^{n} \alpha_i[y_i(\mathbf{w} \cdot \mathbf{x} - b) - 1]\right\}$$

(2.29)

24

which α_i are zero for data points which are outside of the slab bounded by $\mathbf{w} \cdot \mathbf{x} - b = 1$ and $\mathbf{w} \cdot \mathbf{x} - b = -1$ (these boundaries are also represented as $y_i(\mathbf{w} \cdot x_i - b) > 1$) as given in Equation 2.26). Therefore, saddle point of Equation 2.29 should give the minimum $\frac{1}{2}\|\mathbf{w}\|^2$ value. For now, in order to solve this problem standard quadratic programming techniques and the "stationary" Karush Kuhn Tucker condition may be used so that the solution can be expressed as a linear combination of the training vectors.

$$\mathbf{w} = \sum_{i=1}^{n} \alpha_i y_i x_i \tag{2.30}$$

When α_i are greater than zero, it means that the corresponding x_i lie on the margin and they are the support vectors. Therefore, they satisfy $y_i(\mathbf{w} \cdot x_i - b) = 1$. It can be derived offset b as in Equation 2.31

$$\begin{aligned}
\mathbf{w} \cdot x_i - b &= \frac{1}{y_i} \\
\text{since } y_i = +1 \text{ or } -1, \quad \frac{1}{y_i} &= y_i \\
\mathbf{w} \cdot x_i - b &= y_i \\
b &= \mathbf{w} \cdot x_i - y_i
\end{aligned} \tag{2.31}$$

Offset b value represents the center point of the hyperplane separation and its value can be found with only on the single pair y_i and x_i. In order to estimate a more robust value for b, the average value of all of the N_{SV} support vectors is calculated using Eq. 2.32

$$b = \frac{1}{N_{SV}} \sum_{i=1}^{N_{SV}} (\mathbf{w} \cdot x_i - y_i) \tag{2.32}$$

where N_{SV} is the number of support vectors.

Dual form Classification function given in Equation 2.29 can be expressed in unconstrained dual form and the maximum-margin hyperplane can be found. In this

25

form, the classification task is only a function of the support vectors, i.e. the subset of the training data that lie on the margin. Using the fact that $\|\mathbf{w}\|^2 = \mathbf{w}^T \cdot \mathbf{w}$ and substituting Equation 2.30, the equation 2.27 becomes:

$$\frac{1}{2} \sum_{i,j} \alpha_i \alpha_j y_i y_j x_i^T x_j \tag{2.33}$$

and the dual of the SVM reduces to the following optimization problem:

Maximize (in α_i)

$$\sum_{i=1}^{n} \alpha_i - \frac{1}{2} \sum_{i,j} \alpha_i \alpha_j y_i y_j x_i^T x_j = \sum_{i=1}^{n} \alpha_i - \frac{1}{2} \sum_{i,j} \alpha_i \alpha_j y_i y_j k(x_i, x_j) \tag{2.34}$$

subject to

$\alpha_i \geq 0$, $i = 1, ..., n$ and

$$\sum_{i=1}^{n} \alpha_i y_i = 0 \tag{2.35}$$

Here the kernel is defined by $k(x_i, x_j) = x_i \cdot x_j$ and $\mathbf{w}$ can be computed as:

$$\mathbf{w} = \sum_i \alpha_i y_i x_i \tag{2.36}$$

Biased and unbiased hyperlanes   In order to simplify calculation, the SVM hyperplane may be directed at the the origin of the space. These type of hyperplanes are called *unbiased*, where hyperplanes are not necessarily passing through the origin and they are called *biased*. For an unbiased hyperplane, $b = 0$ is setted in the primal form. Thus, Equation 2.31 can be rewritten as in Equation 2.37.

$$\mathbf{w} \cdot x_i - y_i = 0 \tag{2.37}$$

Soft Margin While hard margin is used to find hyperplane between two classes, Vapnik et. al. suggested a modified maximum margin idea that allows for mislabelled examples as in Figure 2.6 for classification purposes [47].
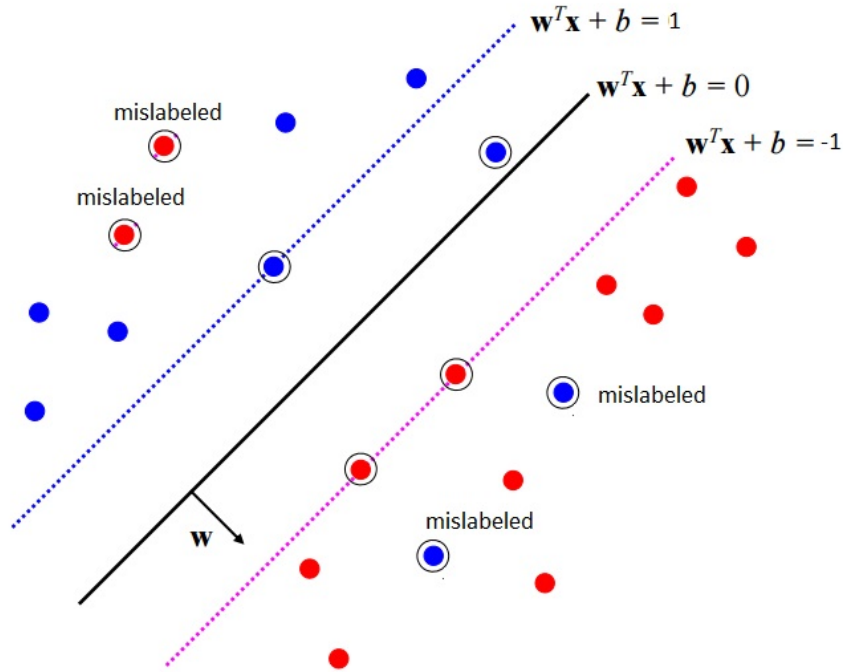
Figure 2.6: Mislabeled Examples

The *Soft Margin* choose a hyperplane that splits the examples as much as possible if there is no hyperplane that can split the two classes perfectly. Yet, the soft margin still maximises the distance to the nearest cleanly split examples. This approach allows large decision margin to make a few mistakes. It is paid a cost for each misclassified example, which depends on how far it is from meeting the margin requirement given in Equation 2.28. In Equation 2.38 ,this method introduces non-negative slack variables, ξ_i, which measure the degree of misclassification of the data x_i [48]

$$y_i(\mathbf{w} \cdot x_i - b) \geq 1 - \xi_i \quad when \quad 1 \leq i \leq n \tag{2.38}$$

The optimization problem is a function which penalizes non-zero ξ_i, and it is trading off between a large margin and mislabelled data points. If the *penalty function* is linear, the optimization problem becomes:

$$argmin_{w,\xi,b}\left\{\frac{1}{2}\|\mathbf{w}\|^2 + C\sum_{i=1}^{n}\xi_i\right\}$$

$$\text{subject to } y_i(\mathbf{w}\cdot x_i - b) \geq 1 - \xi_i$$

$$\text{where } \xi_i \geq 0, \quad \text{for any } i = 1,...,n$$

(2.39)

where C is a *regularization* term. It is observed that if $0 < \xi \leq 1$, it means the data point lies somewhere between the margin and they are labelled correctly and $\xi > 1$, data points are misclassified. This problem can also be expressed as a minimization without constraints:

$$min_w \frac{1}{2}\|\mathbf{w}\|^2 + C\sum_{i} max(0, 1 - y_i(w \cdot x_i - b))$$

(2.40)

In this case, it costs penalty of $C\xi_i$ for the minimization. Upper bound on the number of training errors can be found by the sum of ξ_i. Soft margin SVMs minimize training error traded off against margin. As the parameter C becomes large, it is paid a lot for data points that violate the margin constraint and it is close the hard margin formulation previously described but there is difficulty that it may be sensitive to outlier points in the training data. When C is small, it does not pay that much for points violating the margin constraint. therefore, the cost function can be minimised when $\mathbf{w}$ is chosen as a small norm vector.

This constraint in Equation 2.38 along with the objective of minimizing $\|\mathbf{w}\|$ can be combined to the cost function by using Lagrange multipliers [48] as shown previously:

$$argmin_{w,\xi,b} max_{\alpha,\beta}\left\{\frac{1}{2}\|\mathbf{w}\|^2 + C\sum_{i=1}^{n}\xi_i - \sum_{i=1}^{n}\alpha_i[y_i(\mathbf{w}\cdot x_i - b) - 1 + \xi_i] - \sum_{i=1}^{n}\beta_i\xi_i\right\}$$

$$\text{subject to} \quad \alpha_i, \beta_i \geq 0$$

(2.41)

Dual form for Soft Margin   The dual form of the soft margin is given below.

Maximize (in α_i)

$$\sum_{i=1}^{n} \alpha_i - \frac{1}{2} \sum_{i,j} \alpha_i \alpha_j y_i y_j k(x_i, x_j) \tag{2.42}$$

subject to (for any $i = 1, ..., n$) $0 \le \alpha_i \le C$ and $\sum_{i=1}^{n} \alpha_i y_i = 0$

The use of linear penalty function has an advantage that the slack variables ξ vanish from the dual problem, with the constant C appearing only as an additional constraints on the Lagrange multipliers.

Nonlinear classification   A linear classifier suggested by Vapnik in 1963 [49]. However, in 1992, Vapnik et al.[50] suggested nonlinear classifiers by applying the *kernel trick* to maximum-margin hyperplanes. The nonlinear classifiers is similar to linear one except that a nonlinear kernel function is used instead of inner (dot) product. This allows the algorithm to fit the maximum-margin hyperplane in a transformed feature space. If the transformation is nonlinear, the separating hyperplane in the transformed space $\varphi(x)$ corresponds to a nonlinear surface in the original space x.

For nonlinear SVM, mainly the following kernel functions are used.

Linear Kernel: $k(x_i, x_j) = x_i^T x_j$

Radial Basis Function (RFB): $k(x_i, x_j) = exp(-\gamma \|x_i - x_j\|^d \qquad , \gamma > 0$

Polynomial: $k(x_i, x_j) = (\gamma x_i^T x_j + r)^d, \qquad \gamma > 0$

where γ ,r and d are kernel parameters

The kernel function is related to the transform $\varphi(x_i)$ by the equation $k(x_i, x_j) = \varphi(x_i) \cdot \varphi(x_j)$. The value **w** in Equation 2.36 is also expressed in the transformed space as given in Equation 2.43

$$\mathbf{w} = \sum_{i} \alpha_i y_i \varphi(x_i) \tag{2.43}$$

Since hyperplane in linear space is defined as in Equation 2.23, in nonlinear space hyperplane can be expressed as in Equation 2.44

$$\mathbf{w} \cdot \varphi(x) - b = 0$$
$$\mathbf{w} \cdot \varphi(x) = \sum_i \alpha_i y_i k(x_i, x) - b = 0 \tag{2.44}$$

where k is the kernel function

SVMs is accounted as a generalized linear classifiers. It tries to maximize the margin and minimize the classification error at the same time, therefore SVMs are also called as maximum margin classifiers.

The success of SVM relies on the selection of kernel, the kernel's parameters, and soft margin parameter C. Generally, Gaussian kernel with γ parameters is used. The best suitable selection of γ and C is selected by a *grid search* with exponentially growing sequences of γ and C. These combination is checked using cross-validation methods. Alternatively, Bayesian optimization can also be used to select proper parameters. "The final model, which is used for testing and for classifying new data, is then trained on the whole training set using the selected parameters" [51].

2.3.3   Performance Measures

After applying a classification method, the performance of the classifiers should be measured. Performance is measured by the procedure in which the elements of the population set are each assigned to one of the classes [52]. When all elements are classified as their real class, the best test achieved. A special kind of classification rule which is used mainly also for SVM is binary classification. In simple explanation, binary classification has four component. Assuming two classes, which are positive and negative classes, these four components are explained in the following.

True Positive (TR)   It represents the number of examplars that are classified correctly as positive (i.e. as OCD in our case).

False Positive (FR)   For interested class, the number of false examplars gives false positive.

False Negative (FN)   It represents the number of positive examplars that are classified as negative.

True Negative (TN)   The number of negative examplars classified correctly gives true negative.

With these definitions, positive predictive value (PPV), or precision, for interested class is calculated as:

$$PPV(Precision) = \frac{TP}{TP + FP} \tag{2.45}$$

Also, negative predictive value (NPV) can be calculated for the other class as

$$NPV = \frac{TN}{FN + TN} \tag{2.46}$$

In binary classification, there are two more parameters that represent the results of the classifier. *Sensitivity*, which is also called true positive rate or the recall, is the proportion of positives to all elements in interested class. *Specificity*, which is also called true negative rate, measures the proportion of negatives that are correctly classified. Both sensitivity and specificity equations are given in 2.47.

$$Sensitivity(Recall) = \frac{TP}{TP + FN}$$
$$Specificity = \frac{TN}{FP + TN} \tag{2.47}$$

In order to measure performance of the classifier, *accuracy* or *recognition rate* given in Equation 2.48 is widely used.

$$Recognition\,Rate = \frac{TP + TN}{TP + FN + FP + TN} \qquad (2.48)$$

Also, in statistics F-score value is used to measure test's accuracy. F-score depends on the precision, or PPV, and recall, or sensitivity, which both of them are independent of the number of true negatives:

$$F - score = 2\text{x}\frac{precision\,\text{x}\,recall}{precision\,+\,recall} \qquad (2.49)$$

2.3.4 Cross Validation

Cross validation (CV) is a model validation technique for assessing how the results of a statistical analysis will generalize to an independent data set. CV is generally used in prediction problem. In this problem, a model is trained with known dataset called as *training dataset* and it is tested with unknown dataset called as *test dataset*. The purpose of the cross validation is to define test dataset in order to overcome some generalization errors.

After dividing into two groups, CV technique performs the analysis on the training dataset and the analysis on the test dataset. In order to decrease variability, this partitioning are performed using different datasets and the validation results are averaged.

There is some cross validation technique and one of the is the Leave one out cross validation (LOOCV).

Leave one out cross validation   Leave one out cross validation (LOOCV) uses 1 observation as a test elements and remaining elements as training dataset. The technique repeats its procedure for all elements. Therefore, LOOCV requires to learn and validate C_1^n times where n is the number of observations in the original sample. Since $C_1^n = n$, LOO cross validation does not have the calculation problem of general Leave p out cross validation.

CHAPTER 3

THE DATASET AND EFFECTIVE CONNECTIVITY ANALYSIS APPLIED

3.1 fMRI Experiment and Data Acquisition

In this section, the data set and the fMRI experiment used in this thesis work are explained. The dataset was originally constructed for the study in [2] by the Ankara University, Brain Research Center.

3.1.1 Data Acquisition

The fMRI data was collected with 1.5 Tesla Siemens Magnetom Symphony Maestro Class MRI system (Siemens, Erlangen Germany) by Prof. Dr. Metehan Çiçek and his brain research team in Ankara University, Brain Research Center at Integra Imaging Center, Ankara [2]. There are 79 high resolution images in each one of four sessions acquired with BOLD sensitive T1-weighted functional scans by applying echo-planar sequence. The parameters of imaging are as follows: repeat time (TR)=4940 ms, slice number=36, echo time (TE)=36 ms, slice thickness=5mm, matrix size=64x64, field of view (FOV)=224, flip angle (FA)=90. In order to wait for steady-state magnetisation, the first four images of each session were discarded [2].

33

3.1.2 Participants

The total number of 24 right-handed volunteers with 12 OCD patients (6 female, 6 male) and 12 healthy volunteers. These two groups are matched for gender and level of education. None of the subjects in the control group had neurological disorder or DSM-IV Axis I psychiatric disorder. OCD subjects have abnormalities as three of them checkers, eight of them cleaners and one of them harming obsessions. Disease duration is from 6 months to 7 years. Mean and standard deviation (std) for age, handedness, state anxiety, trait anxiety and Yale-Brown obsessive compulsive scale (Y-BOCS) scores in both groups and P-value for the comparisons of these variables based on student t-test are presented in Table 3.1

Table 3.1: Mean and Standard Deviation of some features of subject [2]

	OCD		Control		P
	Mean	SD	Mean	SD	
Age	27.00	5.80	25.08	3.32	0.331
Handedness	13.33	0.65	13.67	0.89	0.306
State Anxiety	35.17	9.93	31.75	7.66	0.356
Trait anxiety	49.25	8.79	34.50	8.50	0.000
Y-BOCS	20.25	6.24	-	-	-

3.1.3 Experimental Process

A randomly chosen drawing figure as seen in Figure 3.1 was shown to both the OCD patients and control group before they were placed in MRI scanner. Subjects were requested to memorize the figure and before the experiment, they were asked to draw the figure until their drawing fitted correctly. During the experiment, the figure was shown again between scanning sessions to the subjects. In scanning process, they were given verbal command via pre recorded CD. The experiment was done with block fMRI design. There were four main tasks for this experiment and there were four sessions to increase quality of the measured signal. In the first two sessions, suppression task was with imagining, resting and free-imagining task. In suppression task, subjects tried to suppress this figure and think as a blank page. On the other hand, in the last two sessions, erasing task was tried to analyse with imagining, resting and

free-imagining tasks. In this task, subjects were asked to erase the figure starting from the top point as shown with an arrow in previously shown Figure 3.1. The other tasks were used to complete experiment such that the imagining task was for imagination to suppress or erase the drawing; the resting task was for the resting without any imagination and the free imagination task was for the neutral state for the main tasks.
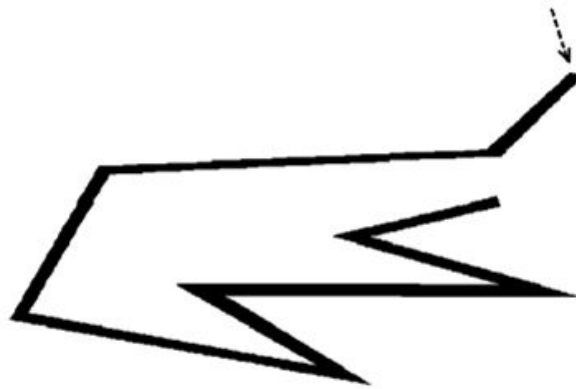
Figure 3.1: The shape used in data acquistion [2]

At the end of the experiment, in first two sessions, there were 60 images for suppression and 30 images for free-imagination. In the same manner, there were 60 images for erasing and 30 images for free-imagination in last two sessions. These images were used to create contrast images such as suppression minus free imagining and erasing minus free imagining. All task was lasted 5 repetition time (TR). The block diagram of the experiment is shown in Table 3.2.

Table 3.2: Block Diagram of Experiment: I: Imagination, S: Suppression, E: Erasing, FI: Free Imagining, R: Resting[2]

Session 1	I	S	R	FI	S	FI	I	S	R	FI	S	R	S	I	S
Session 2	S	R	S	FI	I	S	R	FI	S	I	R	I	S	FI	S
Session 3	I	E	R	FI	E	FI	I	E	R	FI	E	R	E	I	E
Session 4	I	E	R	FI	E	FI	I	E	R	FI	E	R	E	I	E

The results given in study [2] showed that there were small activations on concerned brain regions for erasing task, however only suppression task was better and it is suggested to be used in future studies. Therefore, only suppression task related fMRI data are used in this work.

3.1.4 Preprocessing

The fMRI preprocessing steps necessary after data acquisition are given in Figure 3.2
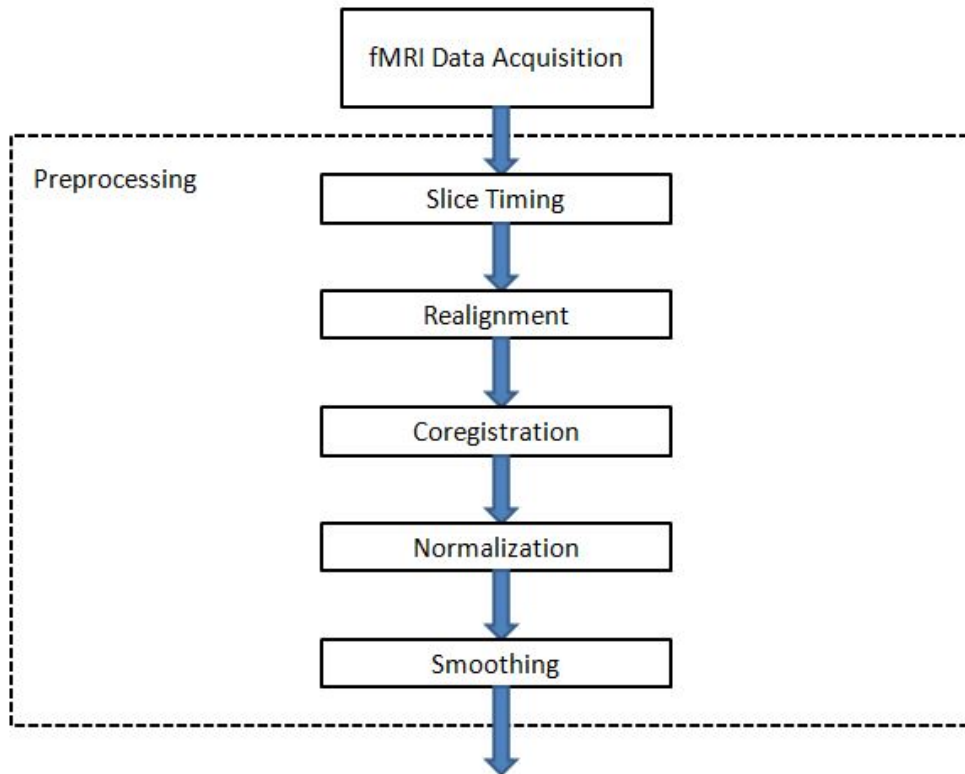
Figure 3.2: Steps considered in Preprocessing

For preprocessing of fMRI data "SPM8 software (Wellcome Trust Center of Neuroimagining)" in MATLAB (Math works, Sherborn, Mass. USA) was used in this study. The user interface of this program for preprocessing is shown in Figure 3.3.

Preprocessing operation consists of five main steps:

(i) *Slice timing*; this step corrects time differences between slices when data was acquired. The aim of this step is to fit all slices to a standard slice in order to equalize time of the activity of each point.

(ii) *Realignment*; this step is used to reduce negative affects of head movements by realigning the fMRI time series to the first frame of image.

Figure 3.3: User interface of SPM8 showing operations for Preprocessing

(iii) *Co-registration*; functional data are of low resolution and are of little anatomical contrast, because of that, data should be mapped onto high-resolution and high-contrast structural images. This step maps the low resolution functional images to high resolution structural images for each subject. Comparison of functional and structural images are shown in Figure 3.4.
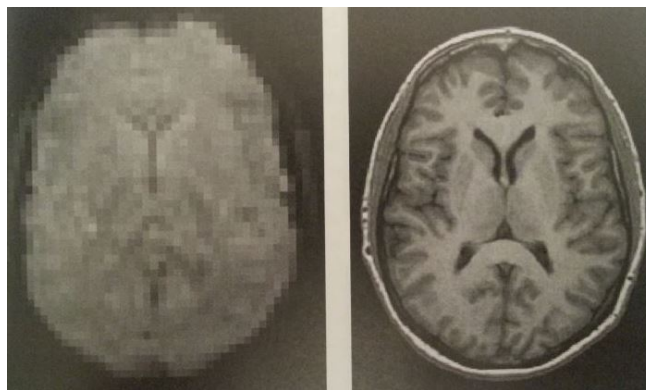
Figure 3.4: Coregistration (a) Low resolution functional images, (b) High resolution images after coregistration [17]

iv) *Normalization*; brain images belonging to different subjects may change in terms of size and shape. In order to compare and group brain images collected from different subjects, these images should be normalized to standard templates. There are two common brain templates called as stereotaxic space; Talairach space and Montreal Neurological Institute (MNI) space [7]. Note that SPM8 uses MNI template.

(v) *Smoothing*; This step increases the signal-to-noise ratio (SNR) by decreasing noise. In order to reduce noise, the functional images are convolved with a Gaussian kernel. In this study, the 6-mm full-width half-maximum (FWHM) Gaussian kernel was used for smoothing. The different smoothing images are given in Figure 3.5.
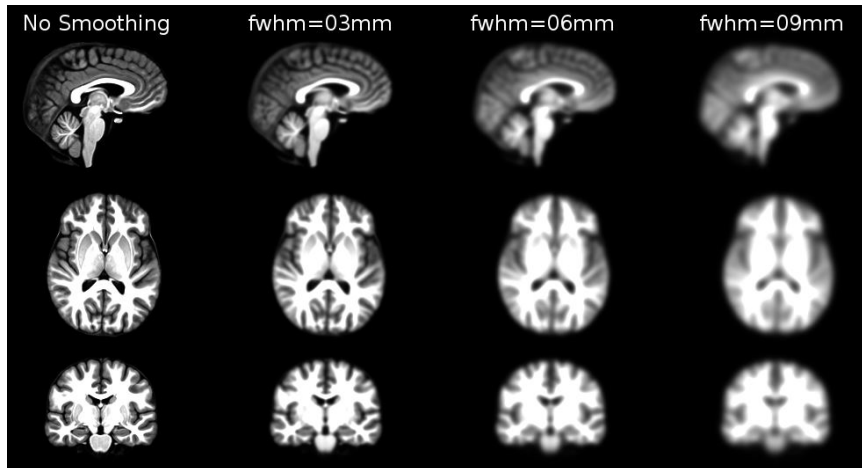
Figure 3.5: Smoothing[7]

3.2 Effective Connectivity Analysis

As stated in Chapter 2, Dynamic Causal Modelling (DCM) is used for effective connectivity analysis to estimate neuronal state parameters by fitting predicted and observed BOLD time series. DCM can be extracted using SPM8 which has special batches for this analysis. SPM8 supports Bayesian Model Averaging (BMA), fixed effect Bayesian Model Selection (BMS) or random effect BMS as well. For this thesis work, random effect BMS analysis was used since there are two different subject classes in the experiment and this type is much more effective than others for group analysis[29].

DCM analysis should start with establishing an optimal neuronal circuit related to the fMRI experiment. This step is first but the most important step for the analysis because DCM results depend on this network. After this step, real time series from the regions of network (volumes) are obtained. After that, DCM estimates the best parameters of circuit on neuronal states. DCM procedure can be summarized as follows

[53]

1) Define a neuronal circuit of contributing regions;

2) Define a model space with different connections within this network;

3) Define the inputs to the network;

4) For each subject, extract BOLD fMRI time series;

5) Estimate the models;

6) Compare all models using the free energy estimate of the model evidence;

7) Compare the leading models, in terms of relevant between-subject factors, using fixed or random methods;

All step are examined in next sections.

3.2.1 The Proposed Neuronal Circuit template for Suppresion task (NC template)

An optimal circuit and possible interactions established based on the significant activations during the suppression task condition. Most of these brain regions were significantly more active in healthy controls than patients. One exception is the insula which was activated significantly both for patients and controls. These coordinates are used to determine where BOLD fMRI time series should be extracted. Dataset used in this work were gathered originally in [2]. After then, this set was also used in [10][13] for OCD signature analysis. The significantly activated regions were Posterior cingulate (PCC, BA 31) , Superior frontal gyrus (SFG, BA 8), Inferior parietal lobe (IPL, BA 40) and Insular cortex (IC, BA 13) by using F-threshold of p<0.05 (corrected). Regions are adjusted to the nearest suprathreshold voxel if there is no voxel above threshold at the specific location for any subject. Table 3.3 summarizes the results of [2] which give activation coordinates on these regions.

Figure 3.6 shows the NC template circuit suggested in this thesis work. This template shows the brain regions which are interested in this work and connections between

Table 3.3: Significant activations observed in [1]

Brain Regions	Cluster size	Laterality	F	Z score	Talairach		
					x	y	z
Inferior parietal lobe (BA 40)	177	R	32.14	4.97	49	-59	40
		R	27.56	4.64	32	-63	35
		R	25.87	4.51	35	-66	45
Superior frontal gyrus (BA 8)	65	R	27.72	4.65	21	40	39
		R	16.36	3.63	18	26	36
Posterior Cingulate (BA 31)	61	R	34.59	5.13	14	-39	34
Insular cortex (BA 13)	112	L	27.44	5.87	-32	7	13
		L	23.44	5.49	-42	-23	20
		L	17.34	4.78	-49	-6	19

them. This network is suggested so that the any combination of given connections creates a new circuit which is used in DCM analysis. The creation of all possible circuit for the analysis is explained in Appendix A and there are 540 different circuits that have been created from this template. These circuits are analysed one by one for DCM and the best fitted one is chosen. From now on, they are called competing models since they are used in DCM analysis.

This proposed template circuit shows that there are intrinsic connections among all regions except that IC and PCC region. Also, suppression is determined as input for this circuit and it only effects on the IC region. Final note from the circuit is that there is no modulatory affects between states. Therefore, in neuronal state equations, there are only A and C parameters for this circuit and using Equation 2.2 in Chapter 2, the neuronal state equations for this circuit are given in Equation 3.1.

$$
\begin{aligned}
\dot{x}_1 &= a_{11}x_1 + a_{12}x_2 + a_{13}x_3 + a_{14}x_4 \\
\dot{x}_2 &= a_{21}x_1 + a_{22}x_2 + a_{23}x_3 \\
\dot{x}_1 &= a_{31}x_1 + a_{32}x_2 + a_{33}x_3 + a_{34}x_4 + c_{21}u \\
\dot{x}_4 &= a_{41}x_1 + a_{43}x_3 + a_{44}x_4
\end{aligned}
\tag{3.1}
$$

These differential equations showing the neuronal state dynamics can be written as given in Equation 3.2
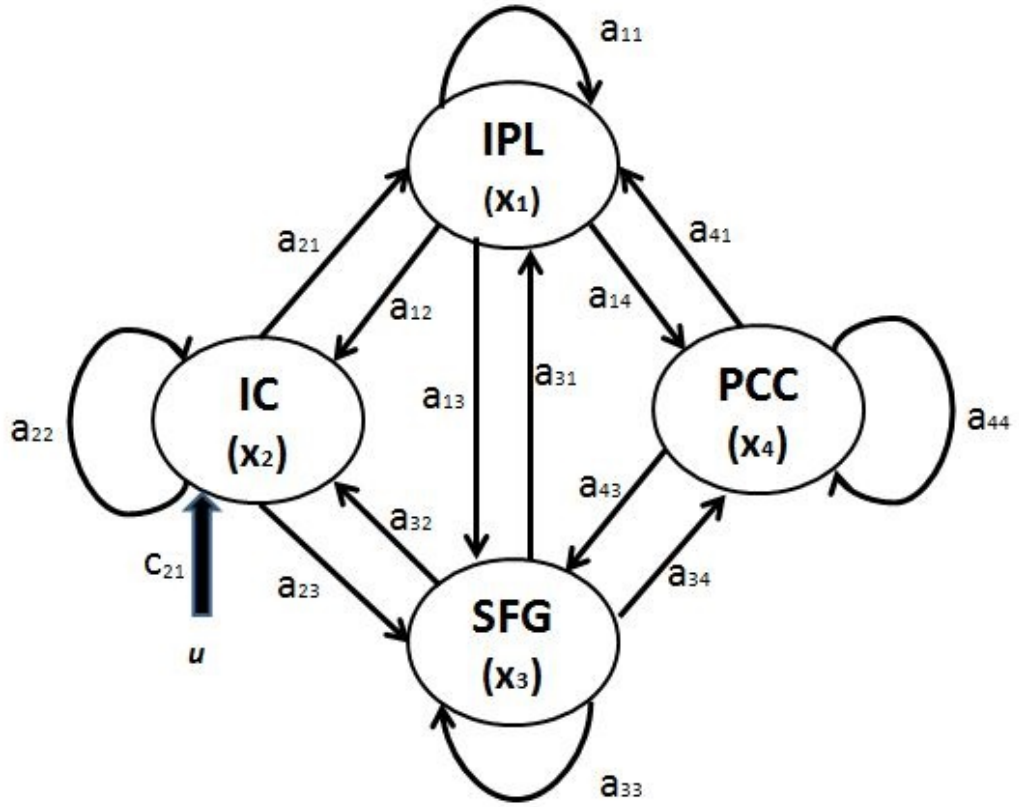
Figure 3.6: The Template Neuronal Circuit proposed for Suppression task

$$
\begin{bmatrix} \dot{x}_1 \\ \dot{x}_2 \\ \dot{x}_3 \\ \dot{x}_4 \end{bmatrix} = \begin{bmatrix} a_{11} & a_{12} & a_{13} & a_{14} \\ a_{21} & a_{22} & a_{23} & 0 \\ a_{31} & a_{32} & a_{33} & a_{34} \\ a_{41} & 0 & a_{43} & a_{44} \end{bmatrix} \begin{bmatrix} x_1 \\ x_2 \\ x_3 \\ x_4 \end{bmatrix} + \begin{bmatrix} 0 \\ c_{21} \\ 0 \\ 0 \end{bmatrix} u \qquad (3.2)
$$

3.2.2 Volume of Interest Extraction

After the neuronal circuit template was proposed, Volume of Interest (VOI) should be extracted. VOI is just a spherical volume that includes voxels. In fMRI, all voxel has their own time series. In functional connectivity analysis, all the time series obtained from each voxel inside the ROI are used. In effective connectivity, a volume is selected with a predefined radius value. Principal Component Analysis (PCA) is

41

applied on the time series of the voxels inside VOI and the resulting principals represent the time series of this volume. These volumes are selected such that the center of them are local maximum in terms of activations. Therefore, VOIs are selected on the regions where activation is occurred and they are used as part of circuit elements. Regions defined in the previous section has volume with activations and VOIs are extracted from these regions by using SPM8. The user interface of VOI is seen in Figure 3.7.
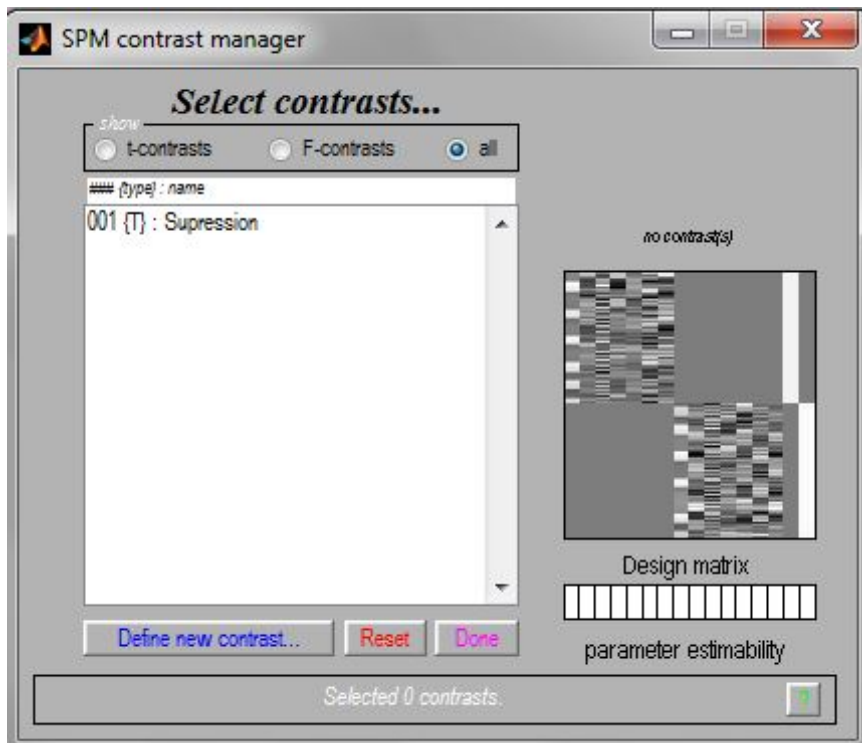
Figure 3.7: The User Interface of VOI Extraction

By using this interface, at first contrast is defined so that it shows only the activation points where contrast is observed. For this study, suppression minus free imagining contrast was used. After that, radius of volume was defined as 8mm (about three voxel size). It is time to choose volumes for the circuit elements. The proposed circuit includes four regions IPL, SFG, PCC and IC and the volumes must be chosen from these regions. In one regions, there is only one time series extracted. Table 3.4 shows the MNI space coordinates where peak activations were detected inside the interested regions.

Now, time series from the volumes are extracted. These data will be used as observed

Table 3.4: The MNI coordinates which have local maximum inside concerned region

	MNI Space of Volumes		
Regions	x	y	z
IPL	48	-62	44
SFG	20	40	42
IC	-34	10	12
PCC	14	-42	36

parameters when DCM estimates yhe neuronal parameters.

3.2.3 DCM Estimations and Bayesian Selections

By now, the possible circuits and their template connections have been determined. There are 540 possible connection combinations and each of them have at least one connection between predefined four regions for suppression contrast data, each of which is corresponding to a competing model. However, the connection values are not determined yet although they are decided to exist or not. DCM estimates what are the connection weights and which of the competitor model has the highest rank.

The DCM was applied for two session which suppression task was used. It is implemented for each subject and for each competitor model based on the template NC. Each model was fitted by SPM8 using expectation maximisation (EM) procedure to estimate intrinsic parameters, input and bilinear connections. DCM also calculates the biophysical model parameters of hemodynamic response fitting to neural activation [24].

In addition to the estimates of the connection parameters, for a competitor model, DCM estimation also derives an estimated log evidence for that competitor model, using negative free-energy criterion as described in Chapter 2. This free-energy shows the accuracy of the model corrected for the complexity of the model. This term depends on both the number of parameters and the dependencies between parameters. Since negative free energy estimates calculates penalty for model complexity as described in Chapter 2, it is used for this thesis work to compare models.

As in Equation 3.2 , the connectivity parameters of proposed network for effective

43

connectivity analysis are found. These parameters also form a connectivity vector as in Equation 3.3

$$\theta = [vec(A) \& vec(C)] \tag{3.3}$$

The estimation results of the negative free energy can be summed over subjects for each model to calculate the estimated cumulative evidence for healthy and patient group. This approach is called as fixed effects method [5] because this method assumes that all subjects generated data from the same neuronal model, without the model itself being a random variable between subjects.

In one session, for each subject, DCM estimates all hidden parameters inside neuronal circuit and hemodynamic model by fitting the calculated signal to measured signal. In this analysis, unlike the past studies that uses Bayes Factor in order to compare the goodness of models, random effect method for group analysis suggested in [25] is used as described also in Chapter 2. As a result of this analysis, the expected posterior probabilities show that how model fits for healthy and patient subject and the exceedance probabilities show that how a model is more likely than one other model. After applying DCM analysis in SPM8, these two results are calculated with Bayesian method and are placed in $BMS.DCM.rfx.model.exp_r$ and $BMS.DCM.rfx.model.xp$ mat file respectively.

After obtaining the exceedance probabilities for the random effect analysis, the circuit with maximum exceedance is the winner circuit. In random effects group analysis, the order of the circuit is the same for all subjects. Therefore, the neuronal circuit parameters can be used for all subjects to compare them.

In this thesis work, healthy and OCD groups have been examined separately. For each group, proposed network template was the input of DCM. After DCM procedure, the exceedance probabilities of competitor models for each are calculated and sorted separately.

The leading models are the best models represent for each group's reaction to the *suppression* task. These reactions are expressed as the effective connectivity and these connectivity parameters are used as the feature vectors of subjects to be classified as

OCD or healthy as explained in the next chapter.

CHAPTER 4

THE PROPOSED METHOD FOR OCD SIGNATURE EXTRACTION

In this chapter, it is explained how the outputs of the DCM analysis is used and converted to the feature vectors for OCD signature extraction and how these feature vectors are used in classification for discrimination of OCD and healthy subjects. There are two steps in this chapter: first step is the *feature extraction* which includes combination of connectivity parameters of DCMs for OCD and healthy subjects together. The other step is the *classification*. Support Vector Machine was used in this study with leave one out cross validation. All details about each process are presented next sections in this chapter.

4.1 Feature Extraction

As stated earlier, the neuronal network parameters, only A and C matrices are expressed as the the effective connectivity among regions. These parameters are estimated from candidate models in DCM analysis by fitting predicted BOLD signals to the observed signals. Since these parameters are dependent to observed BOLD time series, they may also be used as features of each subject. In effective connectivity analysis, subjects performance is determined by two main factors: input and characteristic of individual subjects. As a key aspect of this study, it is assumed that these neuronal state parameters have different distinct values for each subject under the same task analysis and they may be used as features of them to be classified as OCD and healthy.

After the neuronal networks connectivity parameters $\theta(A, C)$ of leading models are found for both class, these parameters are used as features for each subject. The leading models for each group are chosen separately. The θ parameters belong to the subjects from each model become the features of them. The first analysis is done with N leading models for both healthy and OCD groups. The number N is determined intuitively as the best accuracy is reached. These subject's features from both leading models are used for training and testing the classifier. The feature vectors corresponding to subjects are used in training by using Leave-One-Out testing procedure.

The feature creation steps are straightforward but it should be done carefully. In order to create feature vectors for each subject, A and C matrices of the best N circuits should be concatenated. Since the same circuit models are used for all subjects in the same order, i.e., the order of the circuits and their parameters are the same for all subjects, each value in A and C matrices can be compared among subjects. Therefore, only the existing connections in the leading models are used in the feature vectors which means that if there is no connection between any regions, this connectivity parameters can be excluded from the feature vectors.

Feature vectors for first N leading models are created as follows:

1. Take 4 x 4 $A_h^{i,j}$ and $A_p^{i,j}$ matrix for i^{th} model and j^{th} subject , i = 1, 2, ...,N and j = 1, 2, ..., 24 such that A_h represents the A matrix of subjects for leading healthy models and A_p for patient models

$$
A_h^{i,j} = \begin{pmatrix}
a_{h11}^{i,j} & a_{h12}^{i,j} & a_{h13}^{i,j} & a_{h14}^{i,j} \\
a_{h21}^{i,j} & a_{h22}^{i,j} & a_{h23}^{i,j} & a_{h24}^{i,j} \\
a_{h31}^{i,j} & a_{h32}^{i,j} & a_{h33}^{i,j} & a_{h34}^{i,j} \\
a_{h41}^{i,j} & a_{h42}^{i,j} & a_{h43}^{i,j} & a_{h44}^{i,j}
\end{pmatrix}
$$

and

$$
A_p^{i,j} = \begin{pmatrix}
a_{p11}^{i,j} & a_{p12}^{i,j} & a_{p13}^{i,j} & a_{p14}^{i,j} \\
a_{p21}^{i,j} & a_{p22}^{i,j} & a_{p23}^{i,j} & a_{p24}^{i,j} \\
a_{p31}^{i,j} & a_{p32}^{i,j} & a_{p33}^{i,j} & a_{p34}^{i,j} \\
a_{p41}^{i,j} & a_{p42}^{i,j} & a_{p43}^{i,j} & a_{p44}^{i,j}
\end{pmatrix}
$$

2. Take 4 x 1 $C_h^{i,j}$ and $C_p^{i,j}$ matrix for i^{th} model and j^{th} subject , i = 1, 2, ..., N and j =

48

1, 2, ..., 24

$$C_h^{i,j} = \begin{pmatrix} c_{h11}^{i,j} \\ c_{h21}^{i,j} \\ c_{h31}^{i,j} \\ c_{h41}^{i,j} \end{pmatrix}$$

and

$$C_p^{i,j} = \begin{pmatrix} c_{p11}^{i,j} \\ c_{p21}^{i,j} \\ c_{p31}^{i,j} \\ c_{p41}^{i,j} \end{pmatrix}$$

3. Concatenate $C_h^{i,j}$ matrix to last column of $A_h^{i,j}$ matrix to get 4 x 5 $F_h^{i,j}$ matrix and add $C_p^{i,j}$ matrix to last column of $A_p^{i,j}$ matrix to get 4 x 5 $F_p^{i,j}$ for i^{th} model and j^{th} subject , i = 1, 2, ..., N and j = 1, 2, ..., 24

$$F_h^{i,j} = \begin{pmatrix} a_{h11}^{i,j} & a_{h12}^{i,j} & a_{h13}^{i,j} & a_{h14}^{i,j} & c_{h11}^{i,j} \\ a_{h21}^{i,j} & a_{h22}^{i,j} & a_{h23}^{i,j} & a_{h24}^{i,j} & c_{h21}^{i,j} \\ a_{h31}^{i,j} & a_{h32}^{i,j} & a_{h33}^{i,j} & a_{h34}^{i,j} & c_{h31}^{i,j} \\ a_{h41}^{i,j} & a_{h42}^{i,j} & a_{h43}^{i,j} & a_{h44}^{i,j} & c_{h41}^{i,j} \end{pmatrix}$$

and

$$F_p^{i,j} = \begin{pmatrix} a_{p11}^{i,j} & a_{p12}^{i,j} & a_{p13}^{i,j} & a_{p14}^{i,j} & c_{p11}^{i,j} \\ a_{p21}^{i,j} & a_{p22}^{i,j} & a_{p23}^{i,j} & a_{p24}^{i,j} & c_{p21}^{i,j} \\ a_{p31}^{i,j} & a_{p32}^{i,j} & a_{p33}^{i,j} & a_{p34}^{i,j} & c_{p31}^{i,j} \\ a_{p41}^{i,j} & a_{p42}^{i,j} & a_{p43}^{i,j} & a_{p44}^{i,j} & c_{p41}^{i,j} \end{pmatrix}$$

4. Convert $F_h^{i,j}$ and $F_p^{i,j}$ matrix to row vectors successively such that $F_{hv}^{i,j}$ and $F_{pv}^{i,j}$ vectors have 20 elements (1 x 20 matrix)

$$F_{hv}^{i,j} = \begin{pmatrix} a_{h11}^{i,j} & a_{h12}^{i,j} & a_{h13}^{i,j} & a_{h14}^{i,j} & c_{h11}^{i,j} & \dots & \dots & a_{h41}^{i,j} & a_{h42}^{i,j} & a_{h43}^{i,j} & a_{h44}^{i,j} & c_{h41}^{i,j} \end{pmatrix}$$

and

$$F_{pv}^{i,j} = \begin{pmatrix} a_{p11}^{i,j} & a_{p12}^{i,j} & a_{p13}^{i,j} & a_{p14}^{i,j} & c_{p11}^{i,j} & \dots & \dots & a_{p41}^{i,j} & a_{p42}^{i,j} & a_{p43}^{i,j} & a_{p44}^{i,j} & c_{p41}^{i,j} \end{pmatrix}$$

5. Repeat first 4 steps for each model i = 1, 2, ..., N and for specific subject j to create two $1x(20 * N)$ feature vectors of jth subject F_H^j and F_P^j such that

$$F_H^j = \left(\begin{array}{ccccccccc} F_{hv}^{1,j} & F_{hv}^{2,j} & F_{hv}^{3,j} & F_{hv}^{4,j} & F_{hv}^{5,j} & ... & ... & F_{hv}^{(20*N-2),j} & F_{hv}^{(20*N-1),j} & F_{hv}^{20*N,j} \end{array} \right)$$

and

$$F_P^j = \left(\begin{array}{ccccccccc} F_{pv}^{1,j} & F_{pv}^{2,j} & F_{pv}^{3,j} & F_{pv}^{4,j} & F_{pv}^{5,j} & ... & ... & F_{pv}^{(20*N-2),j} & F_{pv}^{(20*N-1),j} & F_{pv}^{20*N,j} \end{array} \right)$$

6. Concatenate F_H and F_P matrix in subject order such that

$$Z = \begin{pmatrix} F_H^1 & F_P^1 \\ F_H^2 & F_P^2 \\ F_H^3 & F_P^3 \\ ... \\ F_H^{23} & F_P^{23} \\ F_H^{24} & F_P^{24} \end{pmatrix}$$

7. Eliminate only the columns in Z matrix if all elements of that column is zero that means there is no connection in the leading circuit corresponding to this parameters. This step increases the accuracy of the classifier by eliminating the parameters where value does not change among subjects. Therefore, each subject has its feature vector which consists of $1x(40 * N - m)$ where m is the total number of no connections.

4.2   Classification

After the feature vectors for each subject are created, classification methods are applied. In order to discriminate patient and healthy subjects from each other, Support Vector Machine (SVM) is used in this study for classification.

4.2.1 Leave One Out Cross Validation

In classification steps, the classifier to be used should be trained and tested carefully. In some studies, obtaining new data separately for testing may not be possible. For obtaining reliable performance results, cross validation is helpful if the data is limited as in the case of this work.

In this study, there are two classes: healthy and OCD patients and from each of these classes, only 12 subject's fMRI records are available. Therefore, a cross validation technique is very suitable for this thesis work. Leave one out is the most suitable technique to convey this experiment. LOO cross validation is summarized as follows:

1. Select one subject as a test subject from Z matrix and remove i^{th} row from this matrix. Use this vector as Z_i^{test} in testing

2. Remaining 23 subjects in Z matrix will be used as the matrix Z_i^{train} in training

The following Figure 4.1 simply shows the Leave one out procedure for 24 subjects.

4.2.2 Support Vector Machine

As stated in Chapter 2, SVM calculates a hyper surface in high or infinite dimensions to discriminate classes from each other. In order to get a good separation, hyperplane should have maximum distance to the nearest data point of any class. Generally, Linear SVM classifier is not suitable for fMRI data because the feature of each subject is formed a vector taking from different models and thus nonlinear SVM is preferred to classify patients from healthy subjects. In SVM classification, Gaussian radial basis function (RBF), polynomial kernel function and linear kernel function are mostly used kernel functions in SVM classification.

According to [36], the Gaussian RBF kernel function is preferred to linear and polynomial one to use in SVM because linear kernel is already the special case of RBF. On the other hand, polynomial kernel may have too many parameters when high order functions are considered. Different kernel functions with different parameters cause different results for classification and choosing the right one and obtaining maximum

Experiment No	Healthy subjects												OCD Subjects											
	S1	S2	S3	S4	S5	S6	S7	S8	S9	S10	S11	S12	S13	S14	S15	S16	S17	S18	S19	S20	S21	S22	S23	S24
1	X	O	O	O	O	O	O	O	O	O	O	O	O	O	O	O	O	O	O	O	O	O	O	O
2	O	X	O	O	O	O	O	O	O	O	O	O	O	O	O	O	O	O	O	O	O	O	O	O
3	O	O	X	O	O	O	O	O	O	O	O	O	O	O	O	O	O	O	O	O	O	O	O	O
4	O	O	O	X	O	O	O	O	O	O	O	O	O	O	O	O	O	O	O	O	O	O	O	O
5	O	O	O	O	X	O	O	O	O	O	O	O	O	O	O	O	O	O	O	O	O	O	O	O
6	O	O	O	O	O	X	O	O	O	O	O	O	O	O	O	O	O	O	O	O	O	O	O	O
7	O	O	O	O	O	O	X	O	O	O	O	O	O	O	O	O	O	O	O	O	O	O	O	O
8	O	O	O	O	O	O	O	X	O	O	O	O	O	O	O	O	O	O	O	O	O	O	O	O
9	O	O	O	O	O	O	O	O	X	O	O	O	O	O	O	O	O	O	O	O	O	O	O	O
10	O	O	O	O	O	O	O	O	O	X	O	O	O	O	O	O	O	O	O	O	O	O	O	O
11	O	O	O	O	O	O	O	O	O	O	X	O	O	O	O	O	O	O	O	O	O	O	O	O
12	O	O	O	O	O	O	O	O	O	O	O	X	O	O	O	O	O	O	O	O	O	O	O	O
13	O	O	O	O	O	O	O	O	O	O	O	O	X	O	O	O	O	O	O	O	O	O	O	O
14	O	O	O	O	O	O	O	O	O	O	O	O	O	X	O	O	O	O	O	O	O	O	O	O
15	O	O	O	O	O	O	O	O	O	O	O	O	O	O	X	O	O	O	O	O	O	O	O	O
16	O	O	O	O	O	O	O	O	O	O	O	O	O	O	O	X	O	O	O	O	O	O	O	O
17	O	O	O	O	O	O	O	O	O	O	O	O	O	O	O	O	X	O	O	O	O	O	O	O
18	O	O	O	O	O	O	O	O	O	O	O	O	O	O	O	O	O	X	O	O	O	O	O	O
19	O	O	O	O	O	O	O	O	O	O	O	O	O	O	O	O	O	O	X	O	O	O	O	O
20	O	O	O	O	O	O	O	O	O	O	O	O	O	O	O	O	O	O	O	X	O	O	O	O
21	O	O	O	O	O	O	O	O	O	O	O	O	O	O	O	O	O	O	O	O	X	O	O	O
22	O	O	O	O	O	O	O	O	O	O	O	O	O	O	O	O	O	O	O	O	O	X	O	O
23	O	O	O	O	O	O	O	O	O	O	O	O	O	O	O	O	O	O	O	O	O	O	X	O
24	O	O	O	O	O	O	O	O	O	O	O	O	O	O	O	O	O	O	O	O	O	O	O	X

Figure 4.1: The diagonal subject is test subject while the others are used for training
O : used for training and X: used for testing

separation are very essential steps. In this study, the Gaussian RBF kernel is determined as the best one. Also, another important parameter, penalty parameter C, should be adjusted properly so that SVM can make maximum separation. In this study, penalty parameter were found empirically by grid search technique so that the classification accuracy is the highest.

SVM classifiers are trained with the training sets that are obtained with LOO cross validation and test sets are used to measure how the classifier discriminates groups.

SVM classifiers were implemented in MATLAB by using *svmtrain* function to train classifier and *svmclassify* function to test the classifier.

Performance of SVM classifier is tested with binary classification test, also known in statistics as classification function. In Chapter 2, *sensitivity*, *specificity*, *recognition*

52

rate and *F-scores* are described. For this study, these terms are defined for the OCD and healthy groups. Sensitivity measures the proportion of true positives for OCD (P_{OCD}) group and specificity measures the proportion of true negative (P_H) for the same group. By using same terminology, (N_{OCD}) and (N_H) represent false positive and false negatives for OCD respectively. Since both group has only 12 subjects, that is $P_{OCD} + P_H = N_{OCD} + N_H = 12$ Equation 2.46 in Chapter 2 becomes:

$$
\begin{aligned}
Sensitivity(recall) &= \frac{P_{OCD}}{12} \\
Specificity &= \frac{P_H}{12} \\
Recognition\,Rate &= \frac{P_{OCD} + P_H}{24}
\end{aligned}
\tag{4.1}
$$

As given in Chapter 2, in order to calculate F-scores, precisions are calculated as:

$$
Precision = \frac{P_{OCD}}{P_{OCD} + N_H}
\tag{4.2}
$$

CHAPTER 5

RESULTS AND DISCUSSIONS

In this thesis work, effective connectivity analysis based on DCM method is applied to the fMRI data of healthy and OCD group. The connectivity parameters are used for discriminating OCD and healthy subjects. This chapter consists of three main sections. In the first section, the results of DCM estimation with model ranking and connectivity parameters are discussed. In the next section, feature vectors for each subject established as defined in Chapter 4 are presented. Finally, classifier results of SVM considering LOO cross validation is given and its results evaluated with binary classification are also presented.

5.1 Results of DCM Estimation and Bayesian Method for Selection

In [41], the random variable analysis has the better results for the group analysis. Therefore, random effects analysis is used to compare models. Random effect analysis (rfx) is obtained in two separate probabilities: expectance and exceedance. Expected rfx and exceedance rfx probabilities are found in the output files of SPM8 *BMS.DCM.rfx.model.exp_ r* and *BMS.DCM.rfx.model.xp* respectively. Connectivity parameters of DCM results are also given under DCM file. Also the log evidence, F values, estimated by negative free energy, which is the trade off between accuracy and complexity, for each model is obtained under the *BMS.DCM.rfx.F* file. F values obtained for 30 leading healthy models and for 30 leading OCD models are given in Figure 5.1 and 5.2 respectively. Note that F values are parametrized according to the best model of each group.
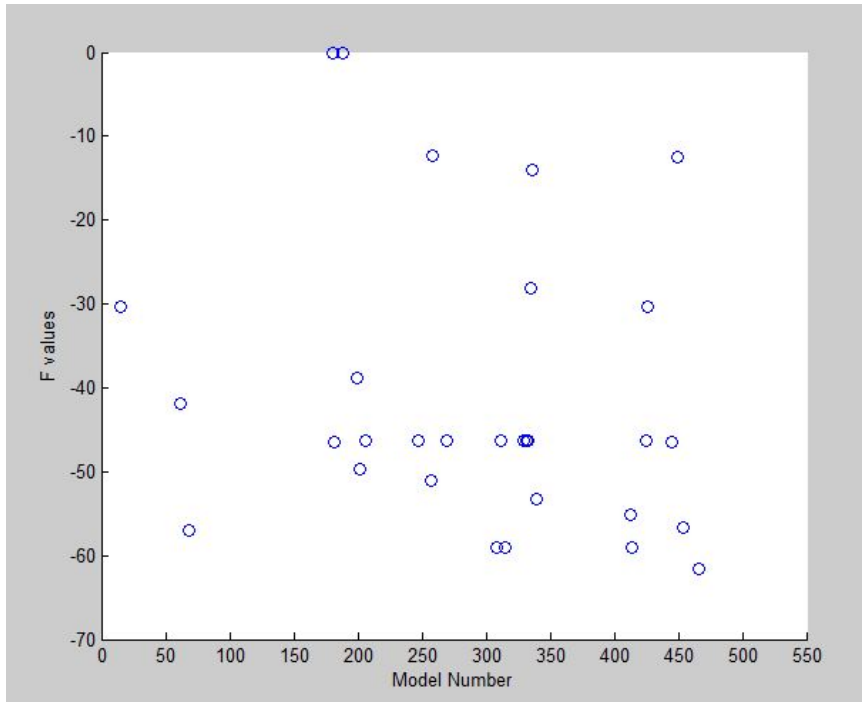
Figure 5.1: F values for the number of models for healthy subjects
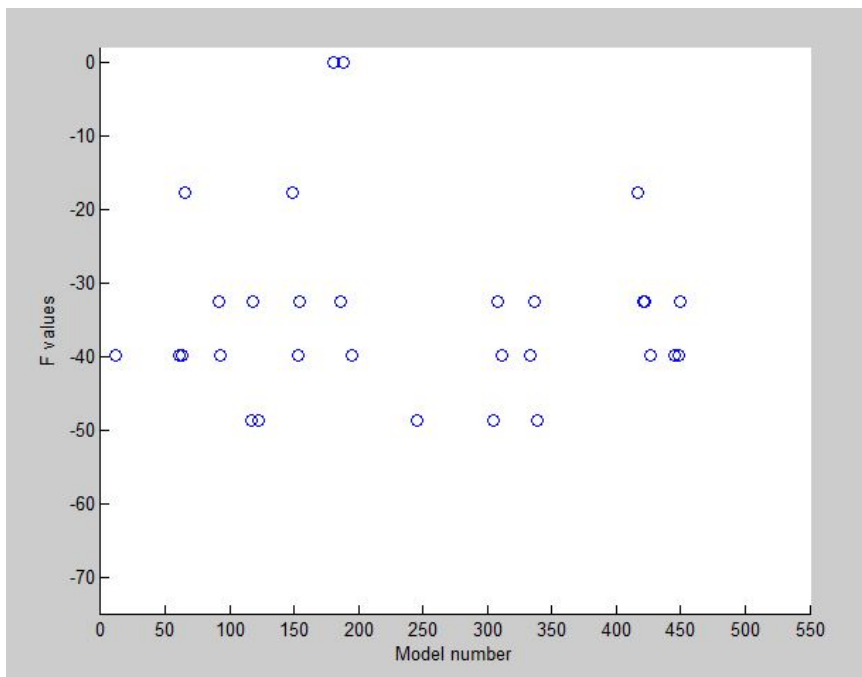
Figure 5.2: F values for the number of models for OCD Patient subjects

According to the F values given in Figure 5.1 and 5.2 , the model with label 181 is the best neuronal network for healthy and the one with label 188 for the OCD. From

now on, these models are called as H181 and P188 respectively for simplicity. In fact H181 and P181 has the same connection in the corresponding competitor model, i.e. model 181, but the values of these connection varies. Note that, each group are analysed within its group with the same order of the models.

It is mentioned in [53] that "...the hierarchical Bayesian model selection approach is equivalent to a random effects analysis incorporating between subject differences in the probability of model having generated the group data." The random effect analysis have two outputs and the competing models are sorted according to these probabilities. Figure 5.3 shows the exceedance probabilities of each competing model for OCD subjects.
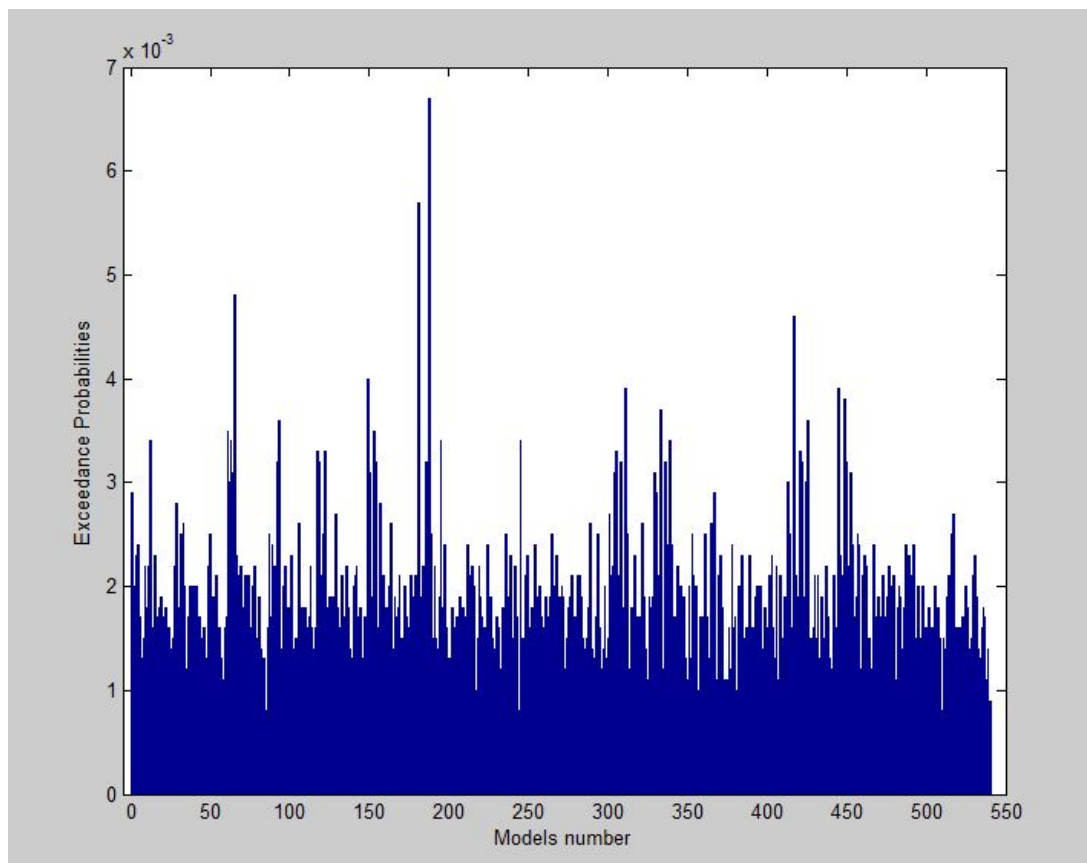
Figure 5.3: Exceedance Probabilities for the number of models for OCD Patient subjects

Also, figure 5.4 shows the exceedance probabilities of each competing model for healthy subjects.
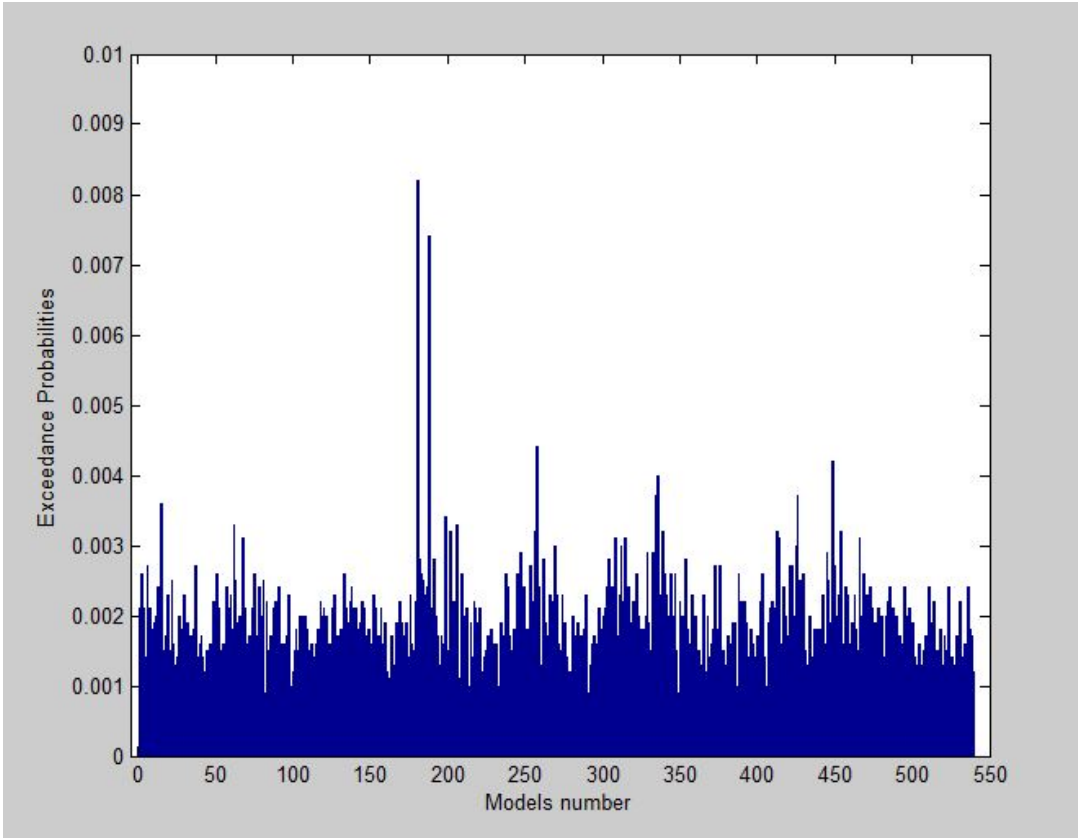
Figure 5.4: Exceedance Probabilities for the number of models for Healthy Patient subjects

For both group, first two models are more likely than other models. The expected and the exceedance probabilities and log evidence (F) values of the first five competing models for OCD and healthy group are given in following tables: Table 5.1 and Table 5.2 respectively.

According to these results, the model with label of 181 is the best model for healthy group (H181) and the model label of 188 is the best model for the OCD group (P188) as we have already found in log evidences. Therefore, the best network, H181 realized from the DCM for healthy group is given in Figure 5.5.

From Figure 5.5, it can be deduced that there is a network starting from IC to PCC connected through IPL and SFG on the brain of healthy people. Representation of the H181 in neural state equations are given in Equation 5.1. It is shown that there are 7 connections among nodes, thus A matrix of this model includes 7 parameters and the

58

Table 5.1: DCM results of best five model for OCD group

	Best Model	2nd Model	3rd Model	4th Model	5th Model
Model Number	188	181	65	417	149
Expected Probabilities (10^{-2})	0.24	0.23	0.21	0.21	0.21
Exceedance Probabilities (10^{-2})	0.67	0.57	0.48	0.46	0.40
F values (relative)	0	2e-06	-17.7	-17.9	-18.1

Table 5.2: DCM results of best five model for healthy group

	Best Model	2nd Model	3rd Model	4th Model	5th Model
Model Number	181	188	258	449	336
Expected Probabilities (10^{-2})	0.25	0.24	0.22	0.22	0.21
Exceedance Probabilities (10^{-2})	0.82	0.74	0.44	0.42	0.40
F values (relative)	0	3e-05	-12.1	-12.8	-13.5

remaining are 0 for no connection. The best model also includes only 1 connection to the input.

$$
\begin{bmatrix} \dot{x}_1 \\ \dot{x}_2 \\ \dot{x}_3 \\ \dot{x}_4 \end{bmatrix} = \begin{bmatrix} a_{11} & 0 & a_{13} & 0 \\ a_{21} & a_{22} & 0 & 0 \\ 0 & 0 & a_{33} & a_{34} \\ 0 & 0 & 0 & a_{44} \end{bmatrix} \begin{bmatrix} x_1 \\ x_2 \\ x_3 \\ x_4 \end{bmatrix} + \begin{bmatrix} 0 \\ c_{21} \\ 0 \\ 0 \end{bmatrix} u \tag{5.1}
$$

For the healthy group, in order to realize connectivity strength, the mean values and standard deviations of each connection for 12 healthy subjects are given in Table 5.3

The same network but analysed among patients (P181) is used for the OCD people. The connection parameters are used for OCD subjects as feature to compare healthy and OCD group. In Table 5.4, mean values and standard deviations of 12 OCD sub-
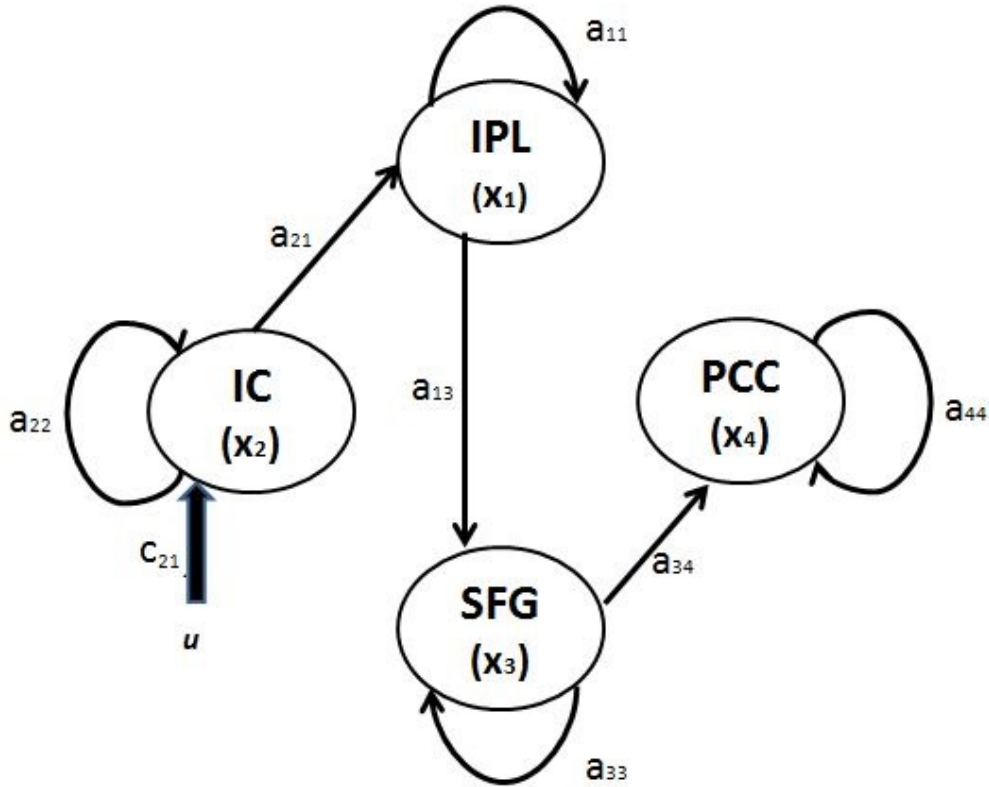
Figure 5.5: The Best Fitted Circuit model for Healthy group

Table 5.3: Means and standard deviations of Healthy group in model H181

connectivity terms:	a_{11}	a_{13}	a_{21}	a_{22}	a_{33}	a_{34}	a_{44}	c_{21}
mean value	-0.2562	0.6253	-0.0051	-0.3000	-0.3181	0.5952	-0.3048	0.0766
std deviation	0.0331	0.0527	0.0100	0.0005	0.0214	0.0393	0.0169	0.0004

jects for the connectivity parameters of the model labelled P181 are given.

Table 5.4: Means and standard deviations of OCD group in model P181

connectivity terms:	a_{11}	a_{13}	a_{21}	a_{22}	a_{33}	a_{34}	a_{44}	c_{21}
mean value	-0.2820	0.6136	0.2065	-0.5997	-0.5066	0.4647	-0.4000	0.0736
std deviation	0.0263	0.0032	0.0062	0.0009	0.0197	0.0099	0.0049	0.0002

In order to show the connection strength differences between healthy and OCD group in healthy leading model H181, Figure 5.6 is given. In this figure, mean value with standard deviations of 12 healthy and 12 OCD group connectivity parameters are

given for the model H181 and P181.
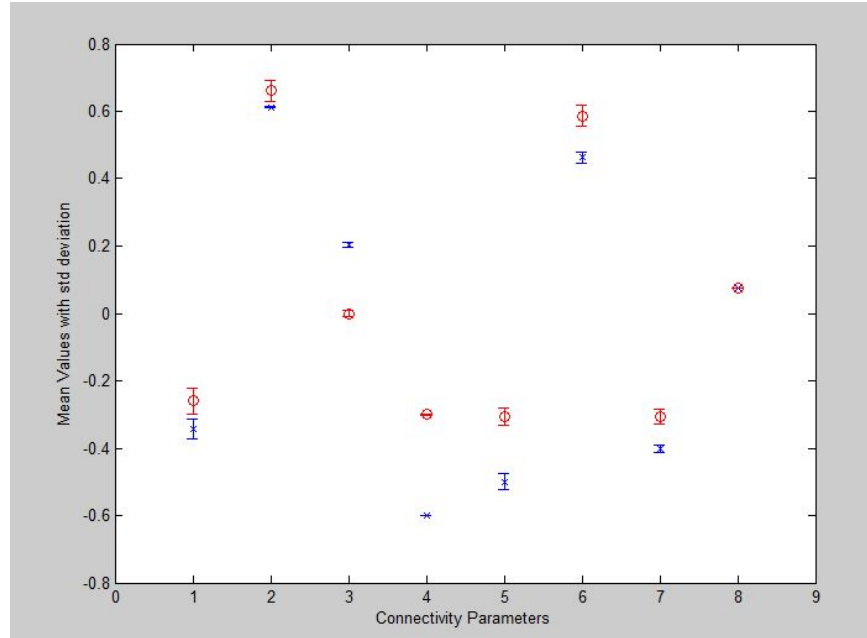
Figure 5.6: Mean values for OCD and healthy subject for the 8 parameters of the best model of healthy subjects ∘ :healthy, x: OCD

In Figure 5.6, there is a clear separation between two class in terms of their mean values and standard deviations of connectivity parameters. Although some parameters for OCD and healthy group are close to each other, many parameters have distant mean and small standard deviations so that they are very effective in discriminating OCD and healthy classes.

On the other hand, for the OCD group, the best fitted model which is the one with label 188 (P188) is given in Figure 5.7.

For the best OCD model, the connection parameters are given in Equation 5.2. It is shown that there are 8 connections among nodes in the best model. Therefore, A matrix of this model includes 8 parameters and the remaining are 0. The best model also includes only 1 connection to the input.

61
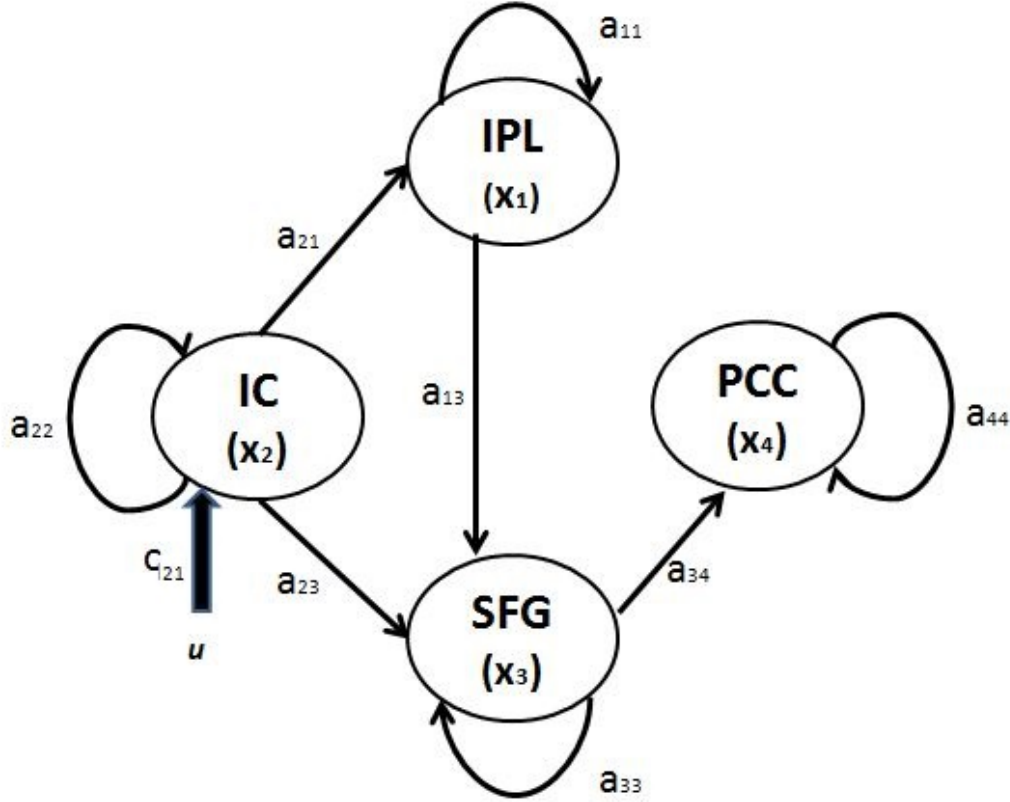
Figure 5.7: The Best Fitted Circuit model for OCD group

$$
\begin{bmatrix} \dot{x}_1 \\ \dot{x}_2 \\ \dot{x}_3 \\ \dot{x}_4 \end{bmatrix} = \begin{bmatrix} a_{11} & 0 & a_{13} & 0 \\ a_{21} & a_{22} & a_{23} & 0 \\ 0 & 0 & a_{33} & a_{34} \\ 0 & 0 & 0 & a_{44} \end{bmatrix} \begin{bmatrix} x_1 \\ x_2 \\ x_3 \\ x_4 \end{bmatrix} + \begin{bmatrix} 0 \\ c_{21} \\ 0 \\ 0 \end{bmatrix} u \qquad (5.2)
$$

For this group, the mean values and standard deviations of 12 OCD subjects for the connectivity parameters are also given in Table 5.5.

Table 5.5: Mean values and standard deviations of OCD group in model P188

connectivity terms:	a_{11}	a_{13}	a_{21}	a_{22}	a_{23}	a_{33}	a_{34}	a_{44}	c_{21}
mean value	-0.4507	0.8144	0.2020	-0.4948	0.2010	-0.2974	0.6596	-0.3072	0.0739
std deviation	0.0309	0.0011	0.0095	0.0015	0.0058	0.0344	0.0201	0.0127	0.0004

The same connection parameters are also important for healthy subjects because these

62

parameters are also used as features to compare healthy and OCD group. At Table 5.6, mean values and standard deviations of 12 healthy subjects for the connectivity parameters of the model labelled H188 are given.

Table 5.6: Mean values and standard deviations of healthy group in model H188

connectivity terms:	a_{11}	a_{13}	a_{21}	a_{22}	a_{23}	a_{33}	a_{34}	a_{44}	c_{21}
mean value	-0.2503	0.4643	0.0020	-0.3021	0.0039	-0.5019	0.3866	-0.5130	0.0765
std deviation	0.0399	0.0033	0.0069	0.0075	0.0056	0.0335	0.0310	0.0129	0.0002

The Figure 5.8 shows the connection strength differences between healthy and OCD group in connectivity parameters of H188 and P188.
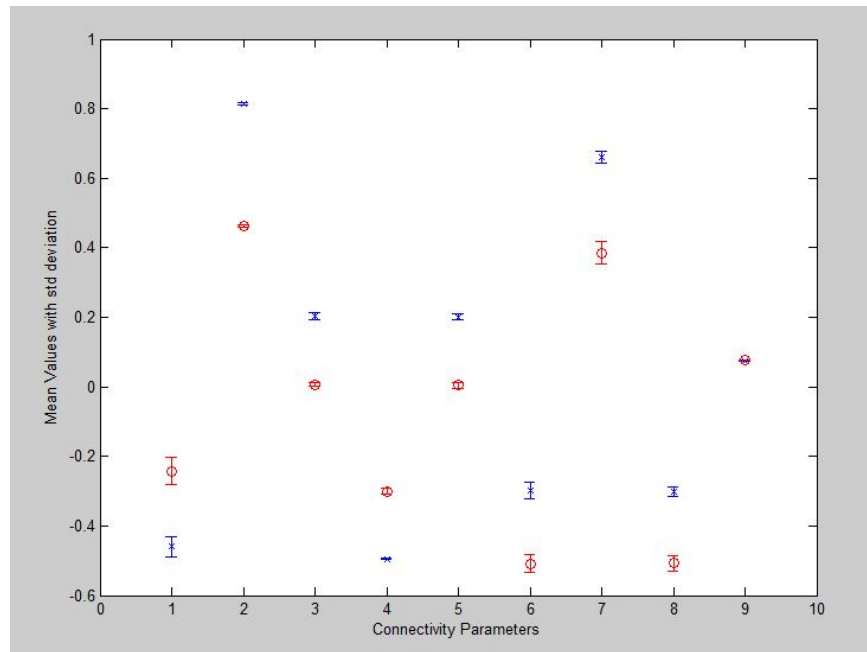
Figure 5.8: Mean values for OCD and healthy subject for the 9 parameters of the best model of OCD subjects ∘ :healthy, ⋄:OCD

The second models are model H188 and model P181 for healthy and OCD group respectively and since these models are the first one for the other group, they already have been used in feature vectors. Also, since they are the same, the classification results are the same with two leading models. The third, fourth and fifth models and their parameters are given in Appendix B.

For the best models, all connectivity values of each subject are given in Figure 5.9.
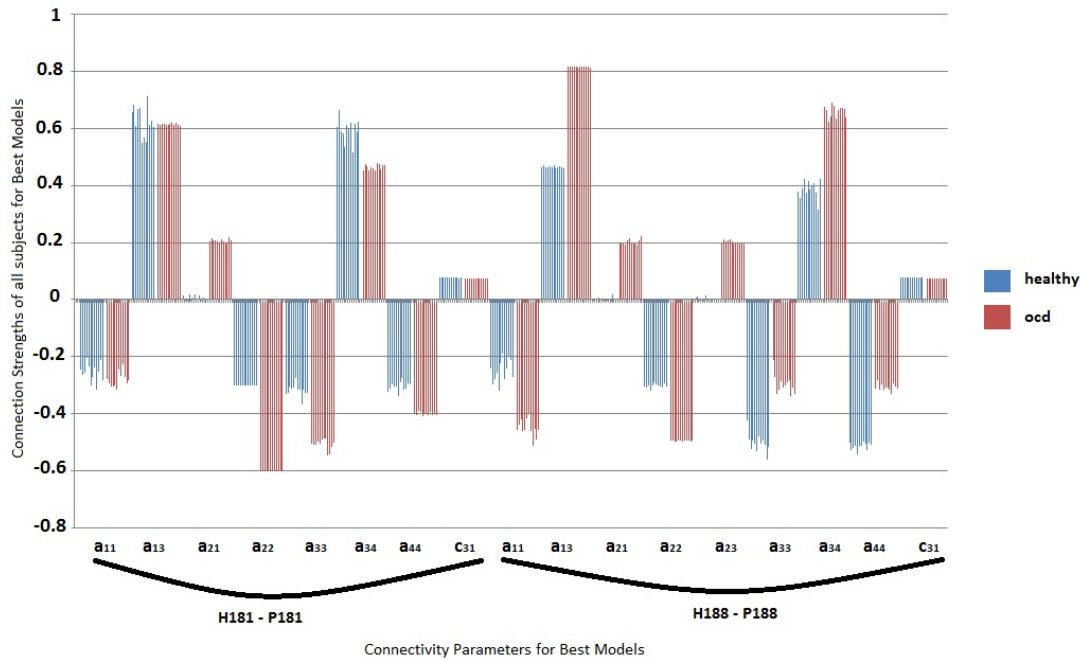
Figure 5.9: Connectivity Strengths of all subjects for the best models

5.2   Results of Feature Extraction

By now, leading two models have been examined. As described in Chapter 4, connectivity vector θ_v for all subjects are created to determine the value of N, which is the number of models to be used in feature vectors. The analysis would be iterative. In order to reduce calculation, only the five models have been examined. In order to create the feature vector for the specific subject, its connectivity parameters for the N leading models for the OCD and healthy cases should be considered.

For $N = 1$, only the best models are taken and the connectivity parameters are found. There are 7 A matrix and 1 C matrix components from best healthy model and 8 A matrix and 1 C matrix components from the best OCD model. Therefore, for $N = 1$, feature vectors for each subject have 17 components.

By the same way, for the first five N values, the feature component numbers are given in Table 5.7. Note that C matrix always contributes 1 component for each model. Since first two models are coincide, the second models have no effective contributions on feature vectors.

64

Table 5.7: The number of Feature Components

N	Model Label of Healthy	Model Label of OCD	Number of feature components from Healthy Model	Number of feature components from OCD Model	Feature vector size of each subject
1	181	188	8	9	17
2	188	181	9	8	17+17=34
3	258	65	11	9	34+20=54
4	449	417	10	9	54+19=73
5	336	149	10	10	73+20=93

5.3 Results of Classifications

5.3.1 Support Vector Machines

As mentioned in Chapter 4, the classification analysis was performed on 24 participants (12 healthy and 12 patient). For training the classifier leave-one-out cross validation is used so that 24 distinct test and train matrix are created.

The SVM classifier is used to discriminate between healthy and patient groups. Since it is suitable much more than other technique, RBF kernel function is preferred in this work. As stated in Chapter 2, RBF kernel parameter (γ) and margin parameter should be selected for the best accuracy. The grid search is used to find best parameters.

Performance of SVM is measured by sensitivity and specificity as described in Chapter 4. The average value of these two values gives recognition rate and it represents the accuracy of the classifier.

After feature vector for each subject is obtained by DCM analysis, Support Vector Machine classification method is applied for first five leading models. For these models, overall SVM results are given in Table 5.8. The best SVM parameters are found with grid search.

Also, the performance results are given in Figure 5.10.

Table 5.8: SVM Performance

N	TP	FP	TN	FN	Sensitivity (%)	Specificity (%)	Accuracy (%)	F-scores
1	11	1	11	1	91.67	91.67	91.67	0.92
2	11	1	11	1	91.67	91.67	91.67	0.92
3	9	3	8	4	75.00	66.67	70.83	0.72
4	8	4	7	5	66.67	58.33	62.50	0.64
5	8	4	7	5	66.67	58.33	62.50	0.64
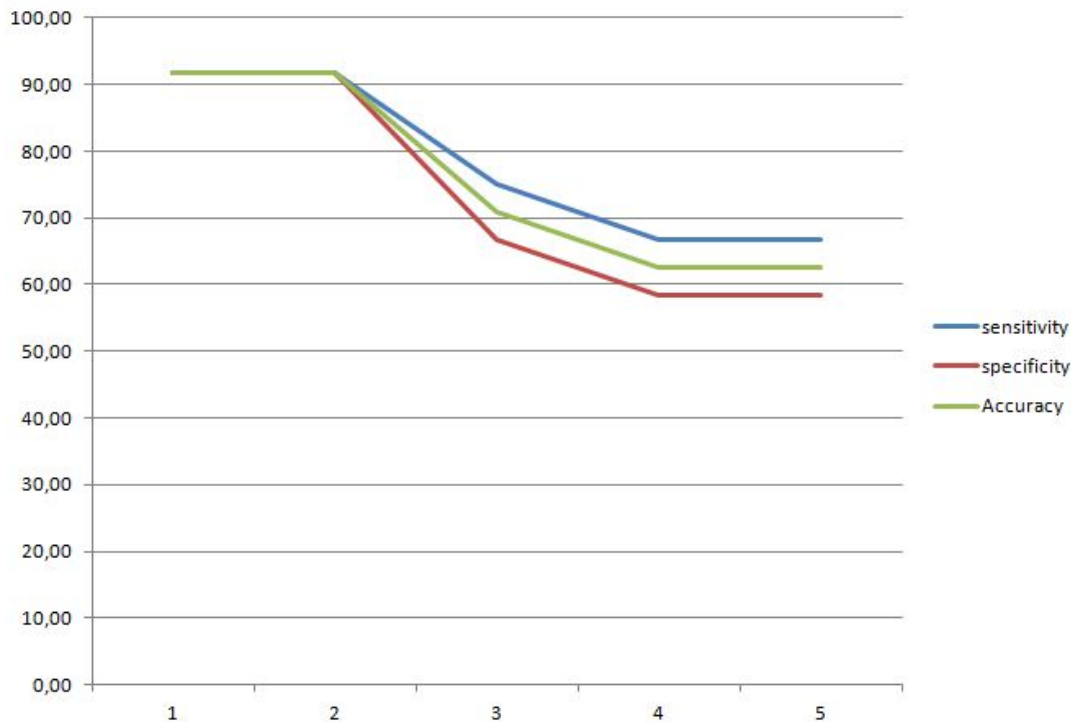
Figure 5.10: Performance of SVM vs number of model

for N=1   In previous section, the connectivity parameters of the best models are converted to the feature vectors for each subject. As shown in Table 5.7 that there are 17 components in the feature vectors for each subjects. LOO cross validation is applied to test each subject and the SVM parameters are tried to find best accuracy.

When only the best model's parameters are used in the feature vector, 1 of 12 OCD subjects and while 1 of 12 healthy subjects are misclassified. This is resulting in 91,67% sensitivity and 91,67% specificity. therefore, this gives 91,67% accuracy. This accuracy is very promising among the studies in literature. The performance

values are summarized in Table 5.8. These results may be improved when the number of models tested increase.

for N=2   Although the best model has a reasonable accuracy to discriminate two groups from each other, this analysis can be extended by using successive leading models as the features of the subjects. When N=2, the first two models' connectivity parameters are used as the features.

As seen in Table 5.2, the exceedance probability of the second model for healthy group is 0.74. This result show that these two models may represent the real activation in hidden states of healthy subjects.

Also as seen in Table 5.1, the best two models for OCD group are compared in terms of their exceedance probability. The second model's probability is about 0.57. This result show that these two models may also represent the real activation in hidden states.

When the best two models of both group are selected so that their connectivity parameters become the features of each subject, the SVM results are as follows: 1 of 12 OCD subjects and 1 of 12 healthy subjects are misclassified. Thus for N=1 and N=2, sensitivity is again 91,67%, specificity is again 91,67% and thus accuracy is 91,67%. Results are again summarised in Table 5.8. This result is not surprising because the feature components are exactly the same with the best models'.

for N=3   Since the first two models' results are very promising, it can be further examined the other successors.

The first three models are compared by their random effect probabilities for healthy and OCD subjects given in Table 5.2 and 5.1 respectively.

As seen in Table 5.2, the exceedance probability of the third model for healthy group is about 0,44.

Also as seen in Table 5.1, the best three models for OCD group are compared in terms of their exceedance probability. The third model's probability is about 0,48.

When the best three models of both group are added to their feature vectors so that their connectivity parameters become the features of each subject. There are 54 components in feature vector for each subject.

In this case, three OCD subjects are misclassified and the other subjects are classified correctly. By using three leading models' parameters as the features, the SVM performance is as follows: sensitivity 75,00%, specificity 66,67% and accuracy is 70,83%. Also, accuracy decreases in comparing to previous results.

In order to see the further results, performance for N=4 and N=5 are given.

for N=4   The first four models are compared by their random effect probabilities for healthy and OCD subjects given in Table 5.2 and 5.1 respectively.

As seen in Table 5.2, the exceedance probability of the fourth model for healthy group is about 0,42.

Also as seen in Table 5.1, the best four models for OCD group are compared in terms of their exceedance probability. The fourth model's probability is about 0,46.

When the best four models of both group are selected so that their connectivity parameters become the features of each subject, there are 73 components in feature vectors.

There are 5 healthy and 4 OCD subjects that are misclassified. The sensitivity decreased to 66,67%, specificity decreased to 58,33% and accuracy decreased to 62,50%. In fact, such a decrease in the performance is not a surprise after some value of N, here N=4, because the successor models do not fit well as the leading ones do, thus they are contributing to the classification but causing unnecessary increase in the feature vector size.

for N=5   The first five models are compared by their random effect probabilities given in Table 5.2 and 5.1 for healthy and OCD subjects respectively.

When the best five models are selected, there are 93 components in feature vector for each subject. In this case, 5 healthy subjects and 4 OCD subjects are misclassi-

fied. Thus, the SVM results are as follows: the sensitivity is 66,67%, specificity is 58,33% and accuracy is 62,50%. These results are also shown in Table 5.8. Thus, the performance of classification for N=5 is very low compared to first two models.

These results show that the best two models have very high accuracy for the discrimination of two groups. When the other successor models have been added to the classification step, the total performances in terms of sensitivity, specificity and accuracy are all decreased. Therefore, it can be deduced that the other successor models will also decrease the quality of discrimination.

When all these performance result obtained in this chapter, the best discrimination is reached when N=1 and N=2, that is the first two models are representing the subjects well to discriminate both groups. The reason for this result is that DCM try to estimate connectivity parameters and the first models' parameters generate very similar signals to the real time series while the rest of the models are not good in representing the subjects.

Furthermore, the performances when the best models used alone are considered. Table 5.9 shows the results obtained when only 181 (best healthy model) and only model 188 (best OCD model) is used. As it is demonstrated in the table, when the best model is applied alone to all subjects, 1 healthy and 1 OCD subjects are misclassified similar with the result of both best models. On the other hand, when the best OCD model 188 is applied to the subjects, all subjects are classified correctly.

Table 5.9: Performace of best models

Model Number	TR	FR	TN	FN	Sensitivity (%)	Specificity (%)	Accuracy (%)
181	11	1	11	1	91.67	91.67	91.67
188	12	0	12	0	100	100	100

CHAPTER 6

CONCLUSIONS

In this study, effective connectivity is used for the first time in literature for disease signature extraction to discriminate OCD subjects from healthy subjects. For this purpose a method is proposed to obtain the feature vector constituting the OCD signature by applying Dynamic Causal Modelling (DCM) on task related fMRI data and the proposed method is tested on data collected from 12 OCD and 12 healthy subjects. These data were used previously in work [13] for the same purpose but the functional connectivity analysis was used instead. For the effective connectivity analysis, Dynamic Causal Modelling (DCM) is applied because the other methods like PPI or SEM are not easily used with event-related data. Also, DCM allows to model a cognitive system at the neuronal level which is not directly accessible from fMRI. In this study, the purpose of applying DCM is to examine effective connectivity among IPL, IC, SFG and PCC brain regions under a suppression task. The parameters of hidden neuronal circuit that represent the effective connectivity among the regions are discovered. These parameters are related directly with measured BOLD time series and they are subject dependent as well as the tasks. Thus, these connectivity parameters are used as the feature of subjects because, by establishing suitable neuronal circuit template. After extracting features for each subject with DCM analysis, Support Vector Machine (SVM) classification method is applied because it is widely used for fMRI data. By the way, in order to obtain feature vectors, not only the best model but also first five models are considered because the leading models also represent the real BOLD time series as much as possible. However, there is a breakpoint that the performance of classification reduces dramatically. By using SVM method, the best discrimination result 91.67% is reached when the first two models' parameters

are used as the feature representing an individual subject to extract OCD signature. This results outcome the previous works on the same dataset. In [10], 72% accuracy was achieved for task related functional connectivity analysis and in [11] the accuracy 69% for resting state functional connectivity fMRI analyses. Furthermore, when the best model parameters are classified separately, 91.67% accuracy is obtained in the best healhty model 181 and 100% accuracy was obtained in the best OCD model 188. Results of this study are supporting the study in [12] which claimed that the effective connectivity is better method than functional connectivity to examine task related activities.

In this study, the model selection is done with random effect analysis because this analysis is better for group studies [38]. Also, the exceedance probabilities of each model are used to compare models. Thus, it can be deduced that these probabilities can be used for model comparison.

This results show that DCM analysis is a very effective way to represent hidden state parameters. This means that the neuronal network of OCD people can be revealed under suppression task. Therefore, these connectivity parameters among IPL, IC, SFG and PCC brain regions can be used to extract OCD Signature.

When the best models for OCD and healthy subject are compared, the only difference lies on the connection from IC to SFG. In healthy people while the SFG is effected from IC through IPL region, there is a shortcut connection from IC to SFG.

In conclusion, the results of this study shows that the effective connectivity parameters obtained by DCM analysis may be used to characterise subjects under a task related fMRI. For future work, these analysis can be applied different kind of OCD or other mental disorders. Also, the neuronal circuit template may be chosen differently to analyse connectivity among the other regions that are not used in this study. Also, the other classification or feature extraction techniques may be used for this thread.

REFERENCES

[1] T. Wolfers, J. K. Buitelaar, C. Beckmann, B. Franke, and A. F. Marquand, "From estimating activation locality to predicting disorder: a review of pattern recognition for neuroimaging-based psychiatric diagnostics,," 2015.

[2] O. M. Koçak, A. Y. Özpolat, C. Atbaşoğlu, and M. Çiçek, "Cognitive control of a simple mental image in patients with obsessive-compulsive disorder," 2011.

[3] S. Ogawa, T. M. Lee, A. R. Kay, and D. W. Tank, "Brain magnetic resonance imaging with contrast dependent on blood oxygenation," 1990a.

[4] C. deCharms, F. Maeda, G. Glover, D. Ludlow, J. Pauly, D. Soneji, J. Gabrieli, and S. Mackey, "Control over brain activation and pain learned by using real-time functional mri," 2005.

[5] K. E. Stephan, N. Weiskopf, P. Drysdale, P. Robinson, and K. Frsiton, "Comparing hemodynamic models with dcm," 2007.

[6] dave Chawla, G. Rees, and K. Friston, "The physiological basis of attentional modulation in extrastriate visual areas," 1999.

[7] S. A. Huettel, A. W. Song, and G. McCarthy, *Functional Magnetic Resonance Imaging*, 2009.

[8] M. Weygandt, C. R. Blecker, A. Schafer, K. Hacicmack, J. D. Haynes, D. Vatil, R. Stark, and A. Schienle, "Fmri pattern recognition in obsessive-compulsive disorder," 2012.

[9] J. S. Abramowitz, S. Taylor, and D. McKAY, "Obssessive compulsive disorder," *Lancet*, 2009.

[10] S. K. Shenas, U. Halici, and M. Cicek, "A comparative analysis of functional connectivity data in resting and task-related conditions of the brain for disease signature of ocd," 2014.

[11] C. Soriano-Mas, J. Pujol, P. Alonso, N. Cardoner, J. M. Menchón, B. J. Harrison, J. Deus, J. Vallejo, and C. Gaser, "Identifying patients with obsessive-compulsive disorder using whole-brain anatomy," 2007.

[12] F. Li, X. Huang, W. Tang, Y. Yang, B. Li, G. J. Kemp, A. Mechelli, and Q. Gong, "Multivariate pattern analysis of dti reveals differential white matter in individuals with obsessive-compulsive disorder." 2014.

[13] S. K. Shenas, "Detection of obsessive compulsive disorder using resting-state functional connectivity data," 2013.

[14] K. J. Friston, "Functional and effective connectivity: A review," 2011.

[15] R. C. Craddock, P. E. Holtzheimer, X. P. P. Hu, and H. S. Mayberg, "Disease state prediction from resting state functional connectivity," 2009.

[16] H. Shen, L. B. Wang, Y. D. Liu, and D. W. Hu, "Discriminative analysis of resting-state functional connectivity patterns of schizophrenia using low dimensional embedding of fmri," 2010.

[17] J. M. R. Cortés and J. Ao, "Feature extraction and classification of a two-class fmri experiment using principal component analysis, lda and svm," 2009.

[18] P. Bey, "fmri analysis using support vector machines," 2012.

[19] Pauling and Coryell, "The magnetic properties and structure of hemoglobin, oxyhemoglobin and carbonmonox hemoglobin," 1936.

[20] N. K. Logothetis, "What we can do and what we cannot do with fmri," 2008.

[21] K. N. Ochsner, S. A. Bunge, J. J. Gross, and J. D. E. Gabrieli, "Rethinking feelings: An fmri study of the cognitive regulation of emotion," 2002.

[22] M. P. van den Heuvel and H. E. H. Pol, "Exploring the brain network: A review on resting-state fmri functional connectivity," 2010.

[23] G. Chen, B. D. Ward, C. Xie, W. Li, Z. Wu, J. L. Jones, M. Franczak, P. Antuono, and S.-J. Li, "Classification of alzheimer disease, mild cognitive impairment, and normal cognitive status with large-scale network analysis based on resting-state functional mr imaging," 2011.

[24] K. J. Friston, L. Harrison, and W. Penny, "Dynamic causal modelling," 2003.

[25] K. E. Stephan and K. J. Friston, "Analyzing effective connectivity with fmri," 2010.

[26] R. Goebel, A. Roebroeck, D. S. Kim, and E. Formisano, "Investigating directed cortical interactions in time-resolved fmri data using vector autoregressive modelling and granger causality mapping," 2003.

[27] K. J. Friston, J. Ashburner, S. J. Kiebel, T. E. Nichols, and W. Penny, *Statistical Parametric Mapping: The Analysis of Functional Brain Images*, 2007.

[28] A. C. Marreiros, S. J. Kiebel, and K. J. Friston, "Dynamic causal modelling for fmri: A two state model," 2008.

[29] K. E. Stephan, L. Kasper, L. Harrison, J. Daunizeau, H. den Ouden, M. Breakspear, and K. J. Friston, "Nonlinear dynamic causal model for fmri," 2008.

[30] K. E. Stephan, W. D. Penny, R. J. Moran, H. E. M. den Ouden, J. Daunizeau, and K. J. Friston, "Ten simple rules for dynamic causal modeling," 2010.

[31] A. P. Smith, K. E. Stephan, M. D. Rugg, and R. J. Dolan, "Task and content modulate amygdala-hippocampal connectivity in emotional retrieval," 2006.

[32] M. L. Seghier, P. zeidman, N. H. Neufeld, A. P. Leff, and C. J. Price, "Identifying abnormal connectivity in patients using dynamic causal modeling of fmri responses," 2010.

[33] W. D. Penny, K. E. Stephan, J. Daunizeau, M. J. Rosa, K. J. Friston, T. M. Schofield, and A. P. Leff, "Comparing families of dynamic causal models." 2010.

[34] M. Desseilles, S. Schwartz, T. T. Dang-Vu, V. Sterpenich, M. Ansseau, P. Maquet, and C. Phillips, "Depression alters "top-down" visual attention: A dynamic causal modeling comparison between depressed and healthy subjects," 2011.

[35] O. David, S. J. Kiebel, L. M. Harrison, J. Mattout, J. M. Kilner, and K. J. Friston, "Dynamic causal modeling of evoked responses in eeg and meg," 2006.

[36] R. B. Buxton and L. R. Frank, "A model for the coupling between cerebral blood flow and oxygen metabolism during neural stimulation," 1997.

[37] K. J. Friston, A. Mechelli, R. Turner, and C. J. Price, "Nonlinear responses in fmri: The balloon model, volterra kernels, and other hemodynamics," 2000.

[38] K. E. Stephan, W. D. Penny, J. Daunizeau, R. Moran, and K. J. Friston, "Bayesian model selection for group studies," 2009.

[39] B. Jin, A. Strasburger, S. J. Laken, F. A. Kozel, K. A. Johnson, M. S. George, and X. Lu, "Featue selection for fmri-based deception detection," 2009.

[40] W. Bian, J. Li, and D. Tao, "Feature extraction for fmri-based human brain activity recognition," 2010.

[41] B. Schuyler, J. M. Ollinger, T. R. Oakes, T. Johnstone, and R. J. Davidson, "Dynamic causal modeling applied to fmri data shows high reliability," 2009.

[42] V. N. Vapnik, *The Nature of Statistical Learning Theory*, 1995.

[43] R. E. Schapire, Y. Freund, P. Bartlett, and W. S. Lee, "Boosting the margin: A new explanation for the effectiveness of voting methods," 1998.

[44] D. D. Cox and R. L. Savoy, "Functional magnetic resonance imaging (fmri) "brain reading": detecting and classifying distributed patterns of fmri activity in human visual cortex," 2003.

[45] S. LaConte, S. Strother, V. Cherkassky, J. Anderson, and X. P. Hu, "Support vector machines for temporal classification of block design fmri data," 2005.

[46] Y. Fan, D. G. Shen, R. C. Gur, R. E. Gur, and C. Davatzikos, "Compare: Classification of morphological patterns using adaptive regional elements," 2007.

[47] C. Cortes and V. Vapnik, "Support vector networks," 1995.

[48] C. D. Manning, P. Raghavan, and H. Schütze, *Introduction to Information Retrieval*, 2008.

[49] V. Vapnik and A. Lerner, "Pattern recognition using generalized portrait method," 1963.

[50] B. Boser, I. Guyon, and V. Vapnik, Eds., *A training algorithm for optimal margin classifiers*, 1992.

[51] W. Hsu, C. Chang, and J. Lin, "A practical guide to support vector classification," 2003.

[52] E. W. Weisstein. (2008) Statistical test. [Online]. Available: http://mathworld. wolfram.com/StatisticalTest.html , last accessed on February 20, 2016

[53] J. Rowe, L. Hughes, R. Barker, and A. Owen, "Dynamic causal modelling of effective connectivity from fmri: Are results reproducible and sensitive to parkinson's disease and its treatment?" 2010.

The template neuronal network has been created based on the previous work. This template network is given in Figure A.1
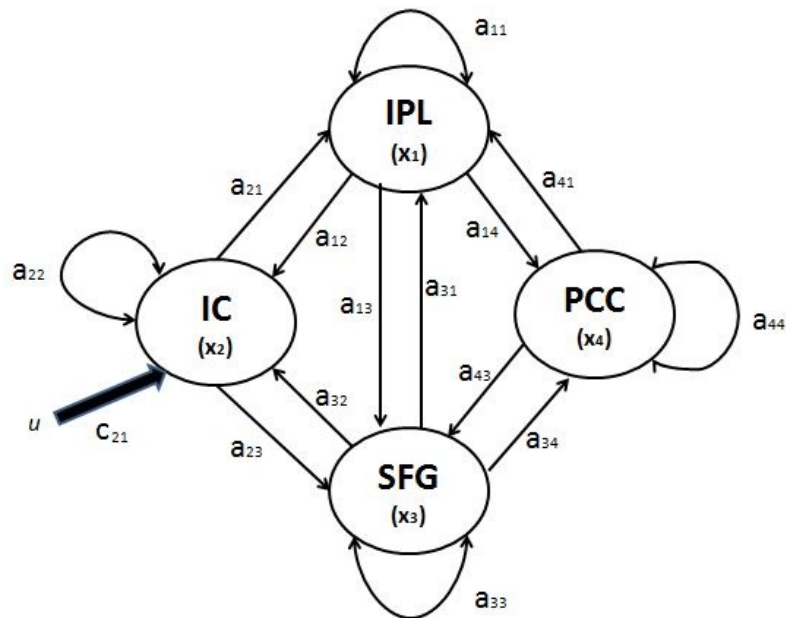
Figure A.1: Template Neuronal Network

In this template network, there are 14 connections. Therefore, it is calculated that there are 2^{14} = 16384 different models could be created. However, this number is too much for DCM analysis because it is actually used for measuring the reactions of proposed brain regions under an examined task. Therefore, this number should be reduced by the expertise on proposed regions. The self loops of all nodes are

preserved for all competing models. Therefore, the first step is to keep all self loops.

The other connections that "must" be available for the analysis in this thesis work are between IPL and IC regions, and IPL and SFG regions. Therefore, at least one connection must be available between IPL and IC regions, and one connection between IPL and SFG regions. In short, there are 9 different models created for these connections that they are called "A type" models. This type of models represent only the mandatory connections between nodes. All of them are not included in analysis but their combinations with other type of models will be used for DCM analysis. Figure A.2 shows type A models.

The other is B type model. These models are interested with the connections between IC and SFG. Since there is at least one connection of IC in either way and at least one connection of SFG in either way due to type A models, type B models can have 4 alternatives as shown in Figure A.3.

The last type models are interested in the connections bounded to the PCC regions. There are $2^4 = 16$ possibilities but one of them is corresponding to no connection. Therefore this model is eliminated and 15 type C models are created as given in Figure A.4.

These three type of models show the possibility of all models that are used for DCM analysis in this work. The competing models are created by all combinations of three type of models. For example, the combination of A1 and B1 and C12 is given in Figure A.5.

Therefore by using all type models, the number of models that are used in DCM analysis are calculated as

$$N = A * B * C = 9 * 4 * 15 = 540 \tag{A.1}$$

One more example for competing models are given in Figure A.6.

To sum up, there are 540 competing models for DCM analysis and they are labelled as 1,2,3...540 by the SPM8. The overall candidate models are given in Figure A.7.
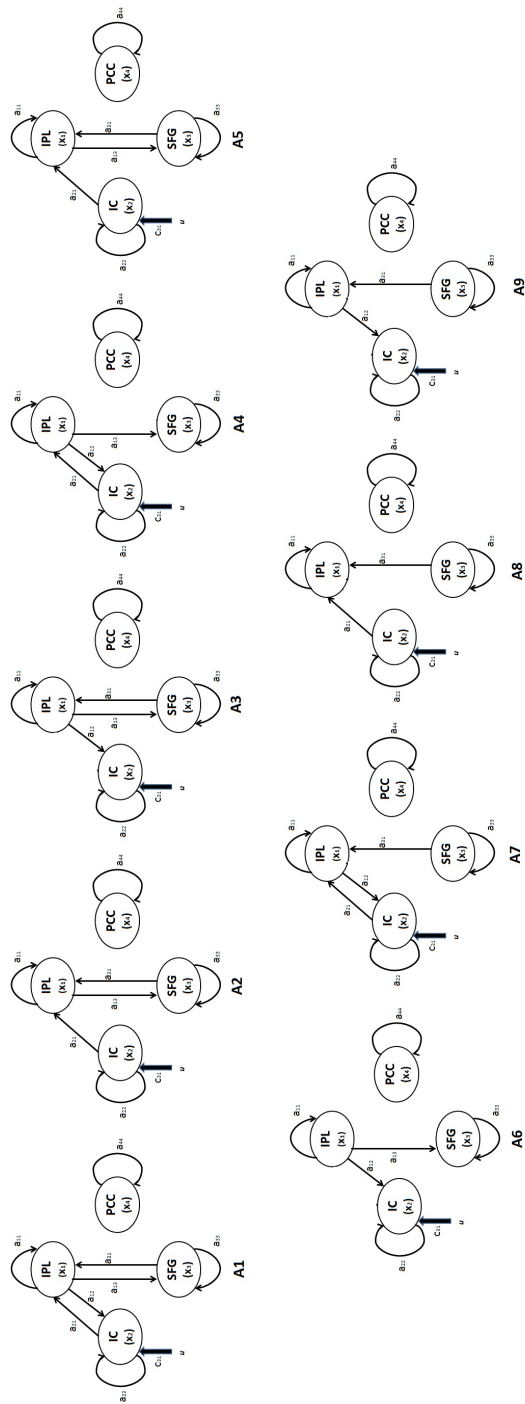
Figure A.2: Type "A" models
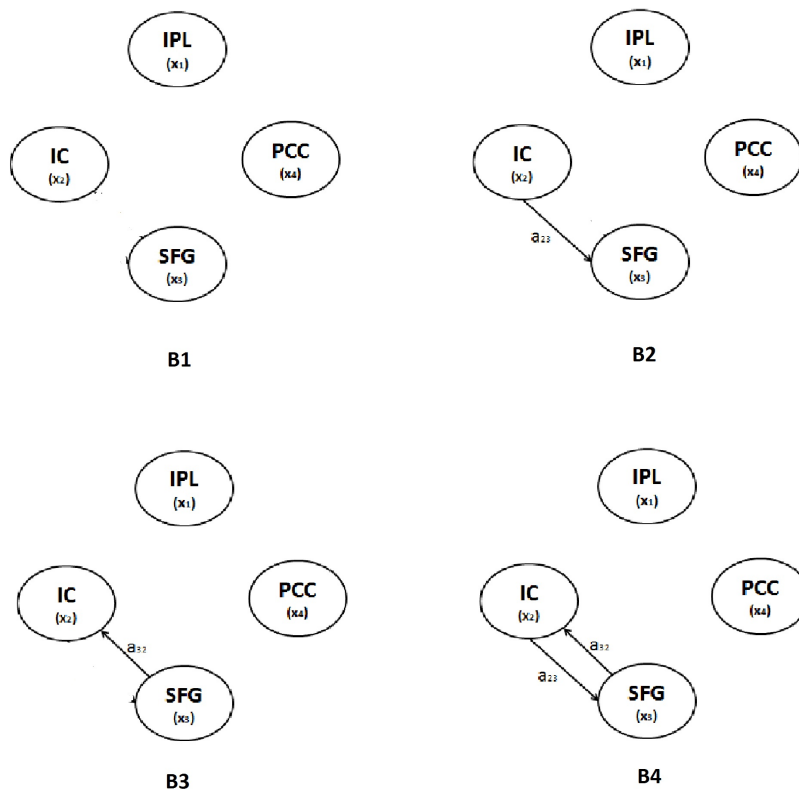
Figure A.3: Type "B" models
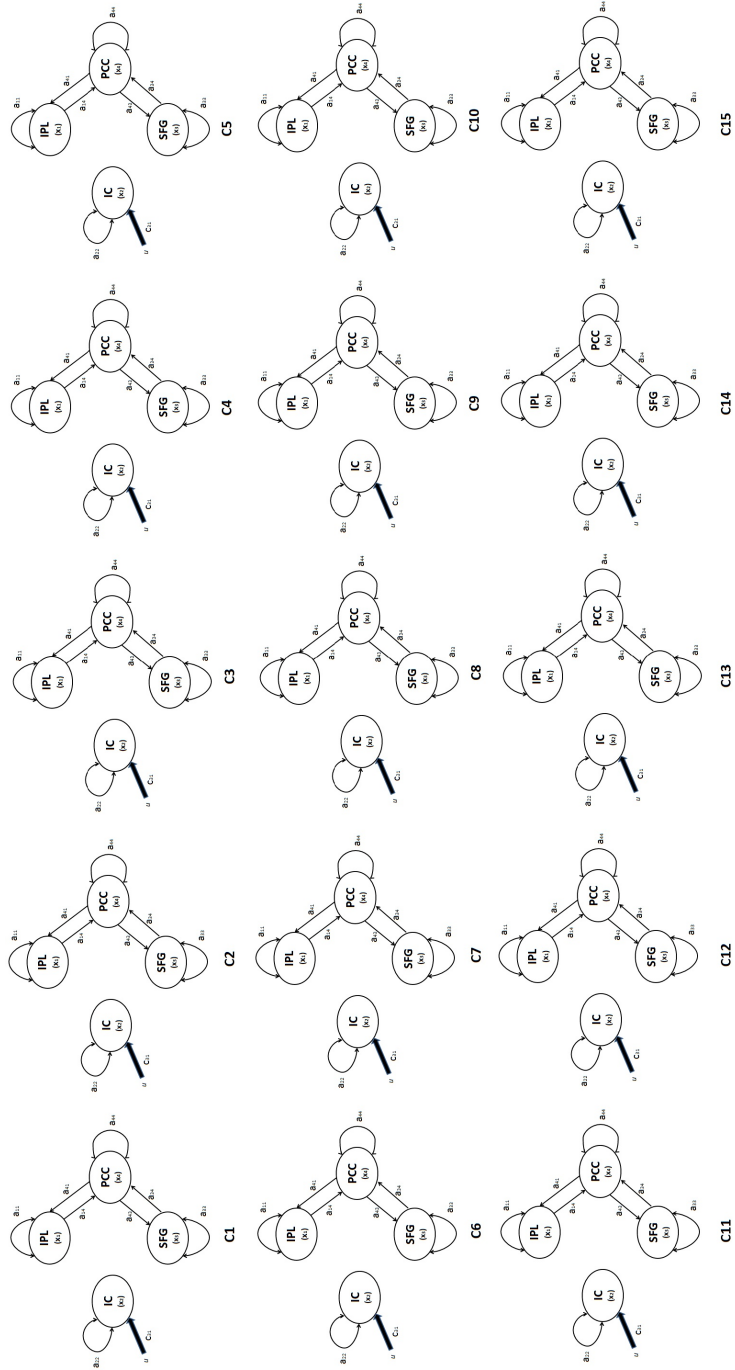
Figure A.4: Type "C" models
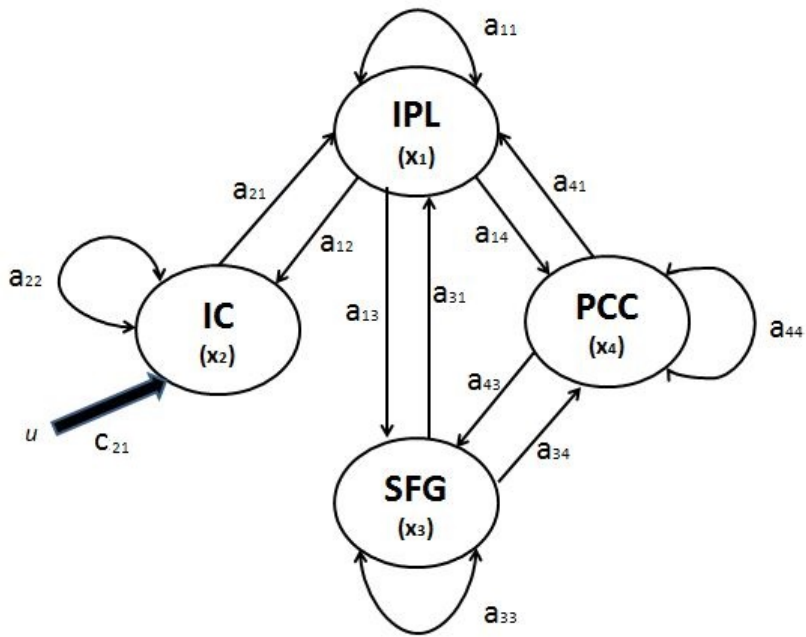
Figure A.5: Combination of A1-B1-C12
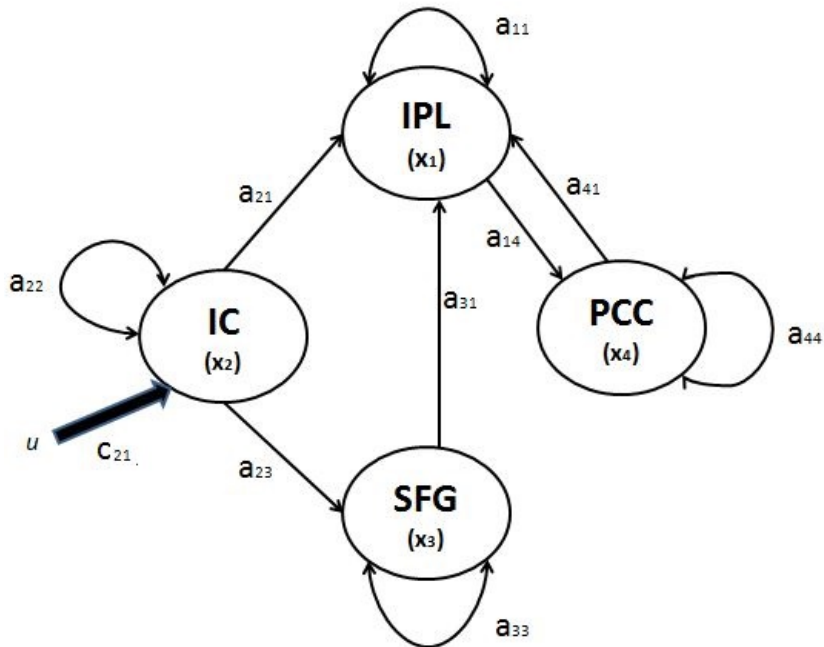
Figure A.6: Combination of A8-B2-C3
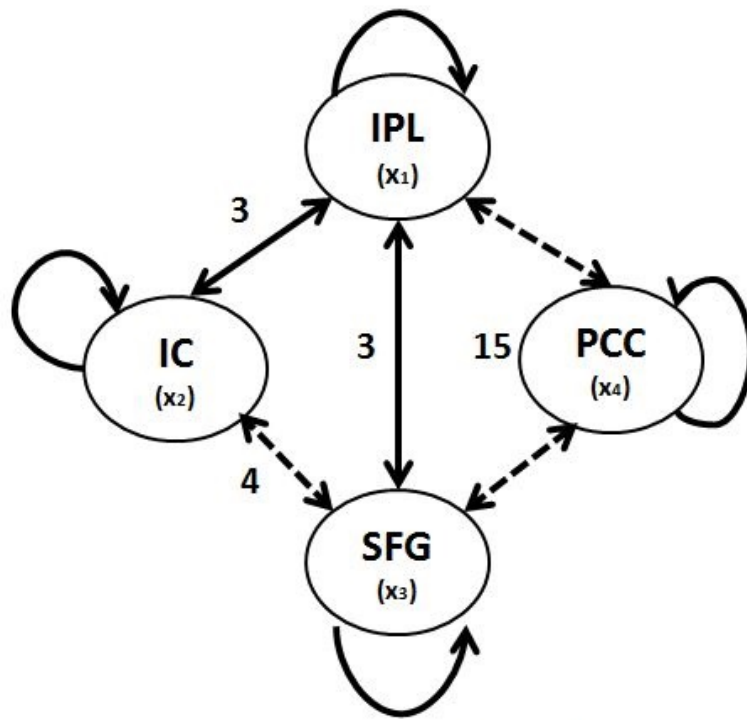
3x3x4x15=540 candidate models

Figure A.7: Combination of all candidate models

APPENDIX B

SUCCESSIVE 3 MODELS

For both group, first and second models are presented in Chapter 5. The following 3 models will be given in this section.

For healthy group, the third model is given in Figure B.9.
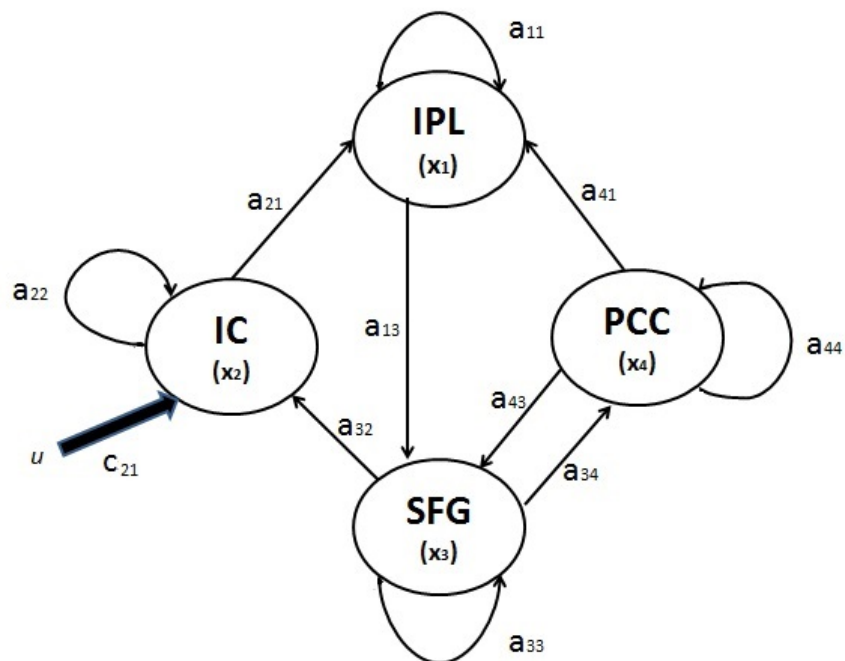
Figure B.1: Third Healthy Model

The matrix representation of this model is given in Equation B.1.

$$
\begin{bmatrix} \dot{x}_1 \\ \dot{x}_2 \\ \dot{x}_3 \\ \dot{x}_4 \end{bmatrix} = \begin{bmatrix} a_{11} & 0 & a_{13} & 0 \\ a_{21} & a_{22} & 0 & 0 \\ 0 & a_{32} & a_{33} & a_{34} \\ a_{41} & 0 & a_{43} & a_{44} \end{bmatrix} \begin{bmatrix} x_1 \\ x_2 \\ x_3 \\ x_4 \end{bmatrix} + \begin{bmatrix} 0 \\ c_{21} \\ 0 \\ 0 \end{bmatrix} u \qquad (\text{B.1})
$$

For healthy group, the fourth model is given in Figure B.10.
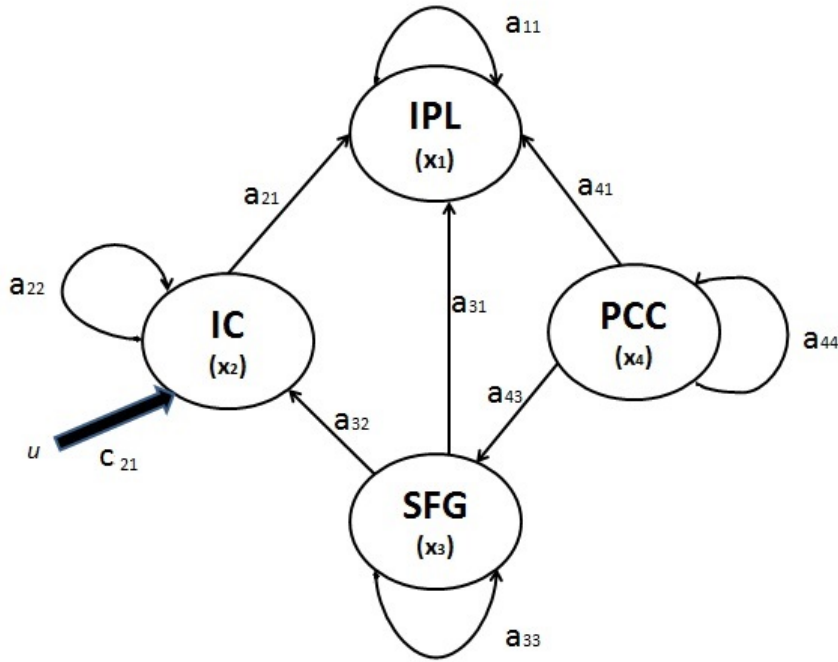
Figure B.2: Fourth Healthy Model

The matrix representation of this model is given in Equation B.2.

$$
\begin{bmatrix} \dot{x}_1 \\ \dot{x}_2 \\ \dot{x}_3 \\ \dot{x}_4 \end{bmatrix} = \begin{bmatrix} a_{11} & 0 & 0 & 0 \\ a_{21} & a_{22} & 0 & 0 \\ a_{31} & a_{32} & a_{33} & 0 \\ a_{41} & 0 & a_{43} & a_{44} \end{bmatrix} \begin{bmatrix} x_1 \\ x_2 \\ x_3 \\ x_4 \end{bmatrix} + \begin{bmatrix} 0 \\ c_{21} \\ 0 \\ 0 \end{bmatrix} u \qquad (\text{B.2})
$$

For healthy group, the fifth model is given in Figure B.11.

The matrix representation of this model is given in Equation B.3.
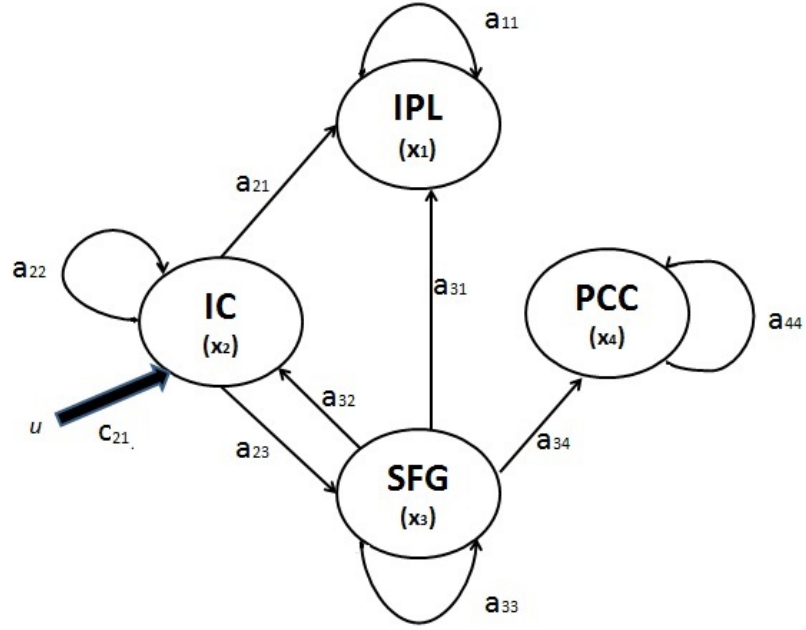
Figure B.3: Fifth Healthy Model

$$
\begin{bmatrix} \dot{x}_1 \\ \dot{x}_2 \\ \dot{x}_3 \\ \dot{x}_4 \end{bmatrix} = \begin{bmatrix} a_{11} & 0 & 0 & 0 \\ a_{21} & a_{22} & a_{23} & 0 \\ a_{31} & a_{32} & a_{33} & a_{34} \\ 0 & 0 & 0 & a_{44} \end{bmatrix} \begin{bmatrix} x_1 \\ x_2 \\ x_3 \\ x_4 \end{bmatrix} + \begin{bmatrix} 0 \\ c_{21} \\ 0 \\ 0 \end{bmatrix} u \qquad (\text{B.3})
$$

For OCD group, the third model is given in Figure B.4.

The matrix representation of this model is given in Equation B.4.

$$
\begin{bmatrix} \dot{x}_1 \\ \dot{x}_2 \\ \dot{x}_3 \\ \dot{x}_4 \end{bmatrix} = \begin{bmatrix} a_{11} & a_{12} & 0 & 0 \\ 0 & a_{22} & 0 & 0 \\ a_{31} & 0 & a_{33} & a_{34} \\ 0 & 0 & a_{43} & a_{44} \end{bmatrix} \begin{bmatrix} x_1 \\ x_2 \\ x_3 \\ x_4 \end{bmatrix} + \begin{bmatrix} 0 \\ c_{21} \\ 0 \\ 0 \end{bmatrix} u \qquad (\text{B.4})
$$

For OCD group, the fourth model is given in Figure B.5.

The matrix representation of this model is given in Equation B.5.

87
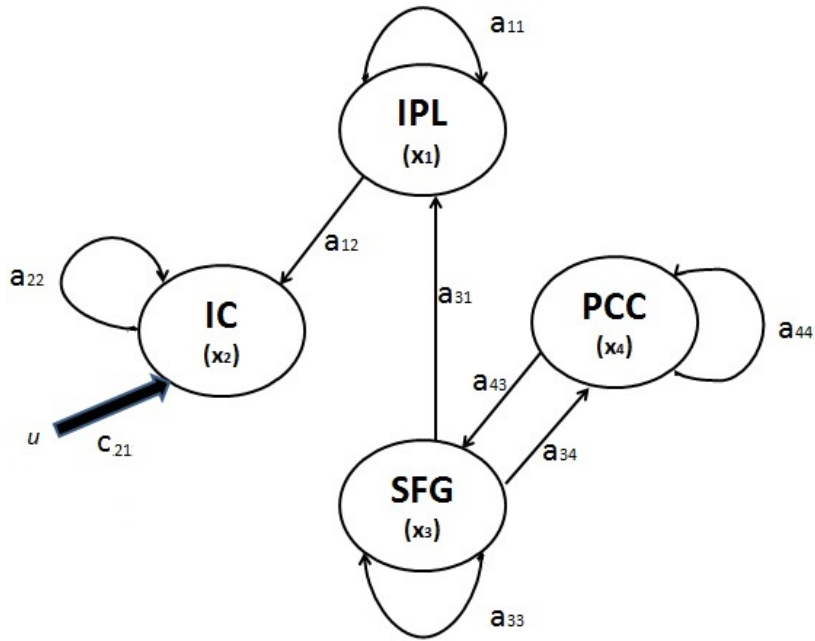
Figure B.4: Third OCD Model
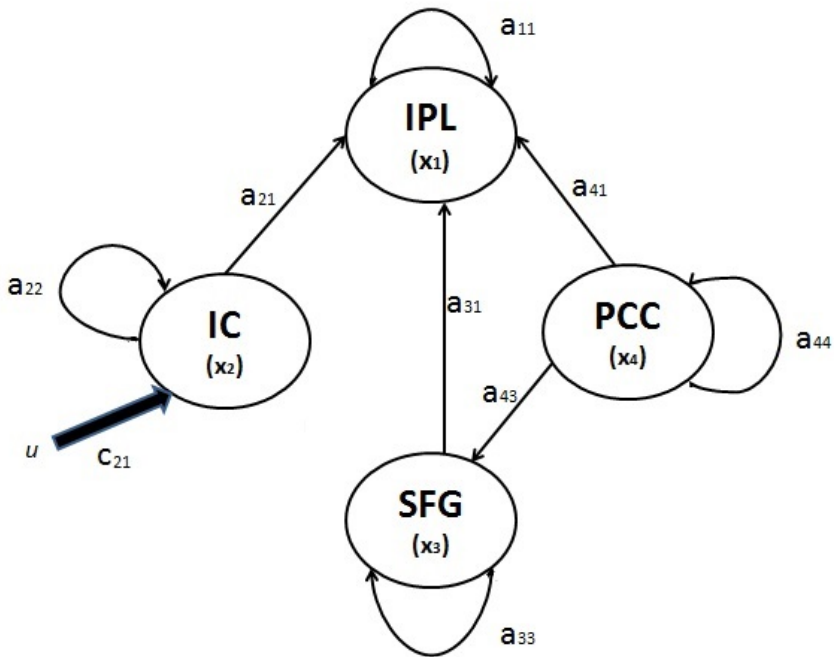
Figure B.5: Fourth OCD Model

$$
\begin{bmatrix} \dot{x}_1 \\ \dot{x}_2 \\ \dot{x}_3 \\ \dot{x}_4 \end{bmatrix} = \begin{bmatrix} a_{11} & 0 & 0 & 0 \\ a_{21} & a_{22} & 0 & 0 \\ a_{31} & 0 & a_{33} & 0 \\ a_{41} & 0 & a_{43} & a_{44} \end{bmatrix} \begin{bmatrix} x_1 \\ x_2 \\ x_3 \\ x_4 \end{bmatrix} + \begin{bmatrix} 0 \\ c_{21} \\ 0 \\ 0 \end{bmatrix} u \qquad (B.5)
$$

For OCD group, the fifth model is given in Figure B.6.
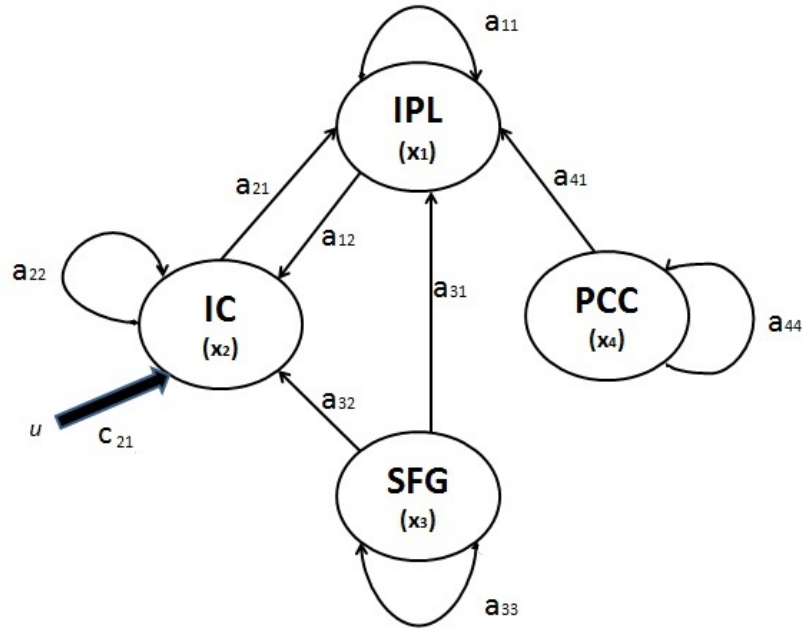
Figure B.6: Fifth OCD Model

The matrix representation of this model is given in Equation B.6.

$$
\begin{bmatrix} \dot{x}_1 \\ \dot{x}_2 \\ \dot{x}_3 \\ \dot{x}_4 \end{bmatrix} = \begin{bmatrix} a_{11} & a_{12} & 0 & 0 \\ a_{21} & a_{22} & 0 & 0 \\ a_{31} & a_{32} & a_{33} & 0 \\ a_{41} & 0 & 0 & a_{44} \end{bmatrix} \begin{bmatrix} x_1 \\ x_2 \\ x_3 \\ x_4 \end{bmatrix} + \begin{bmatrix} 0 \\ c_{21} \\ 0 \\ 0 \end{bmatrix} u \tag{B.6}
$$

Along with the 3 successive models, the connection strengths of each subject in the best models are given in following figures. In these figures, $a_{ij}h$ represents the connection from i to j in the best healthy model and $a_{ij}p$ represents the same node connection in the best OCD model.
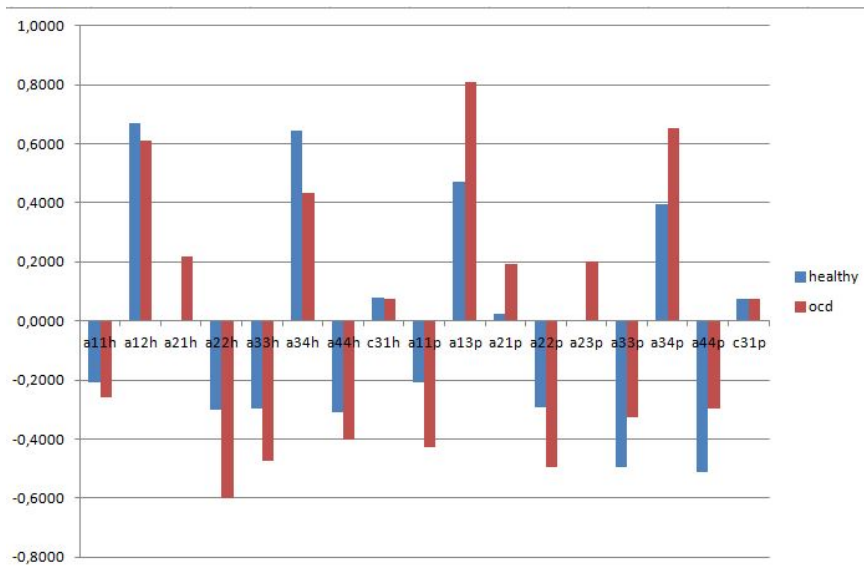
Figure B.7: Connectivity parameters of Subject 1 for best models H181 and P188
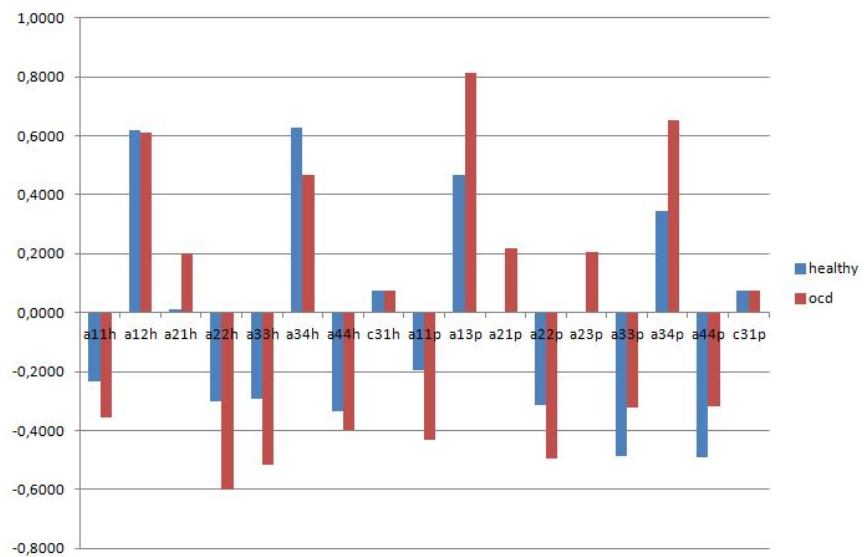
Figure B.8: Connectivity parameters of Subject 2 for best models H181 and P188
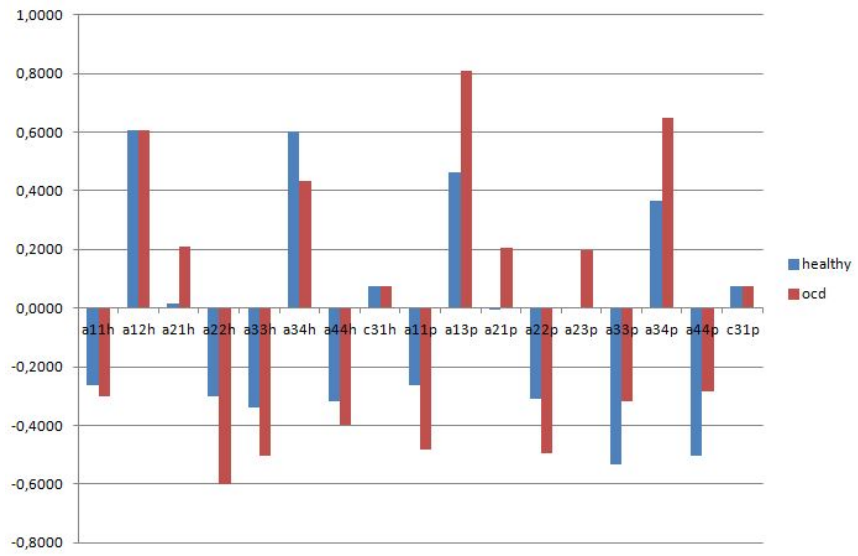
Figure B.9: Connectivity parameters of Subject 3 for best models H181 and P188
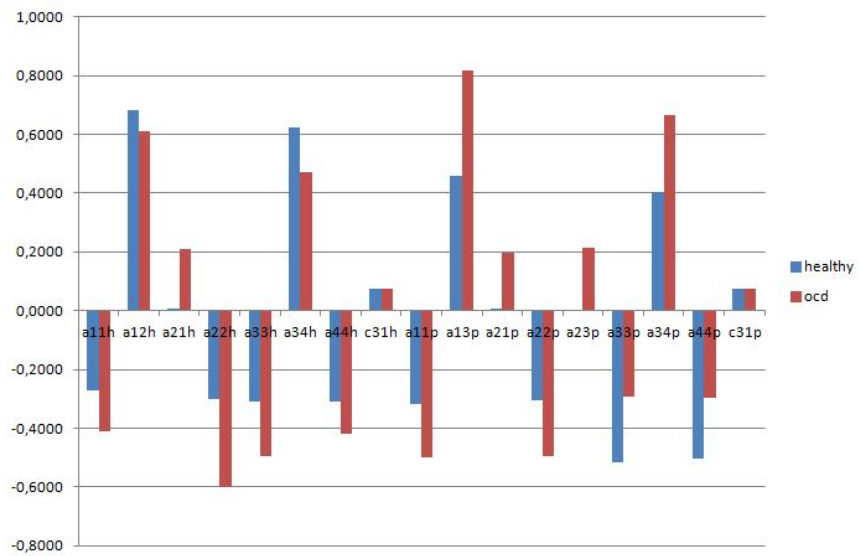
Figure B.10: Connectivity parameters of Subject 4 for best models H181 and P188
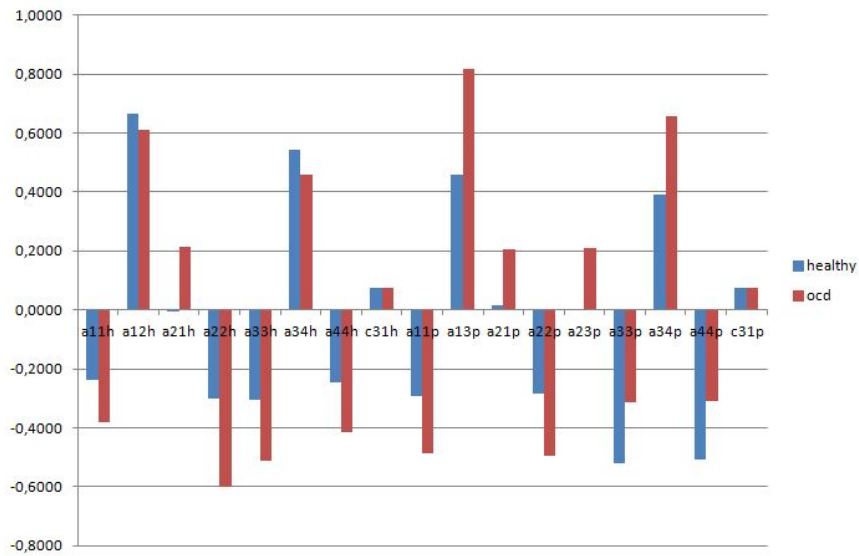
Figure B.11: Connectivity parameters of Subject 5 for best models H181 and P188
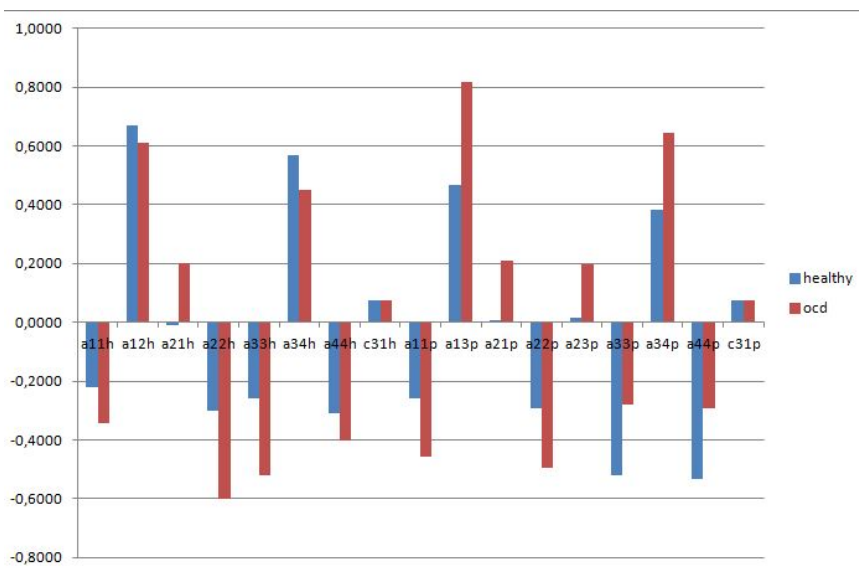
Figure B.12: Connectivity parameters of Subject 6 for best models H181 and P188
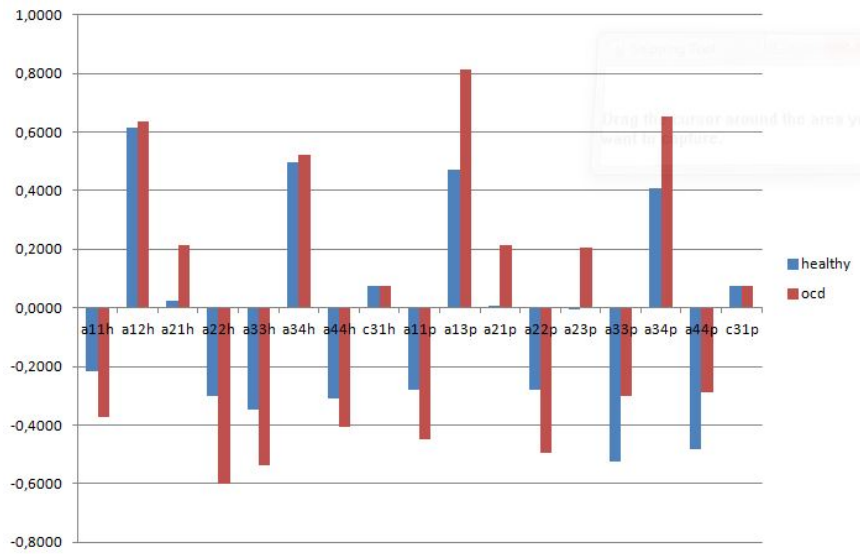
Figure B.13: Connectivity parameters of Subject 7 for best models H181 and P188
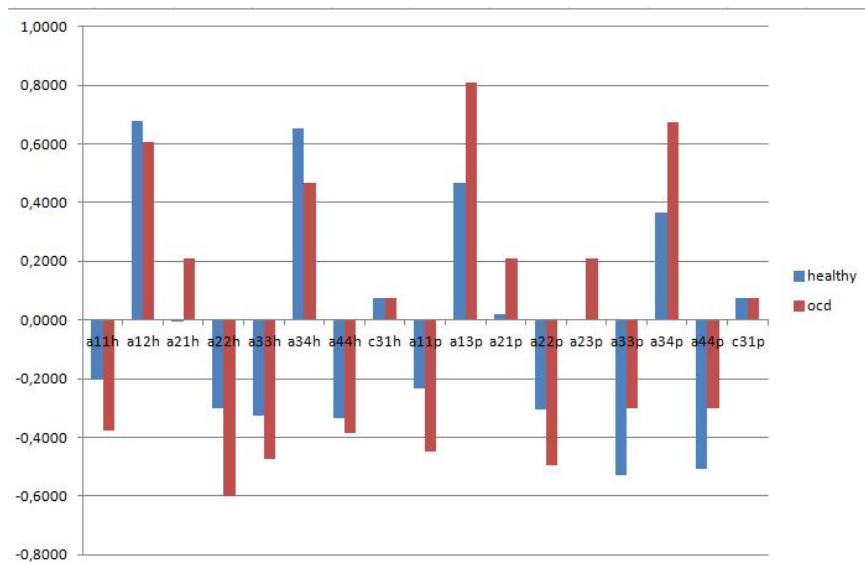
Figure B.14: Connectivity parameters of Subject 8 for best models H181 and P188
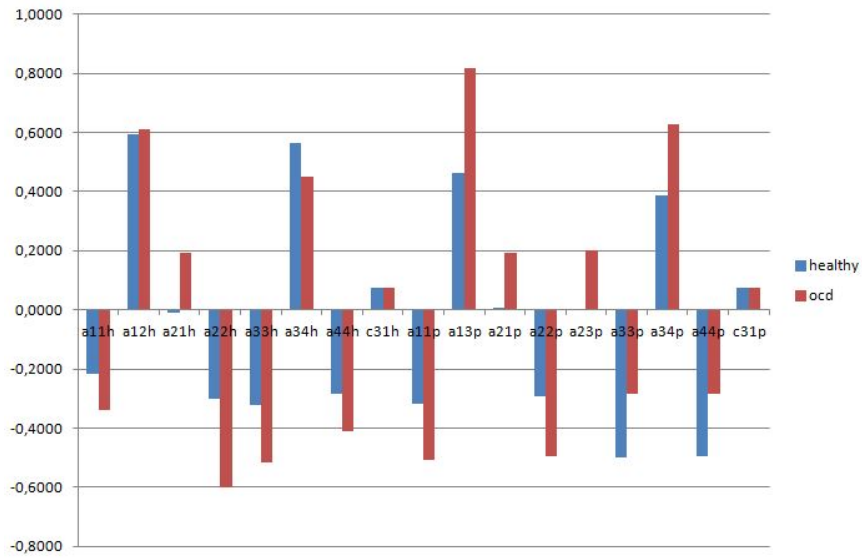
Figure B.15: Connectivity parameters of Subject 9 for best models H181 and P188
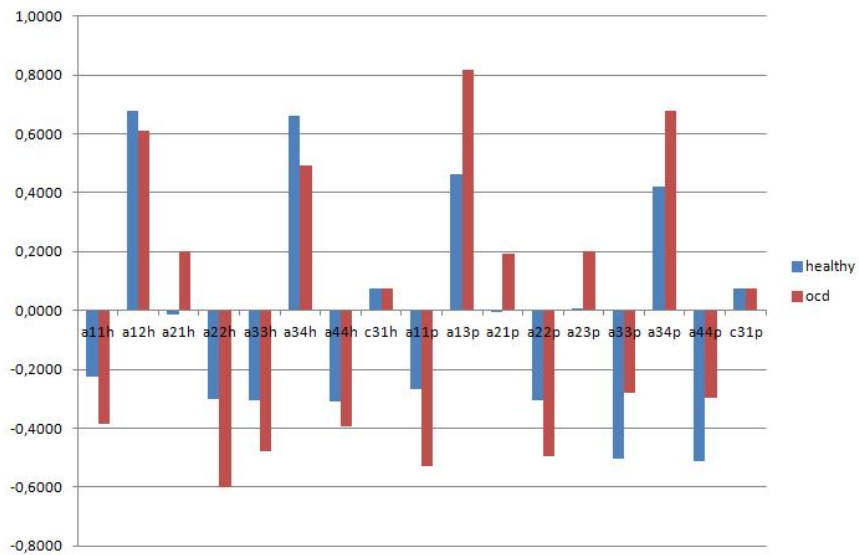
Figure B.16: Connectivity parameters of Subject 10 for best models H181 and P188
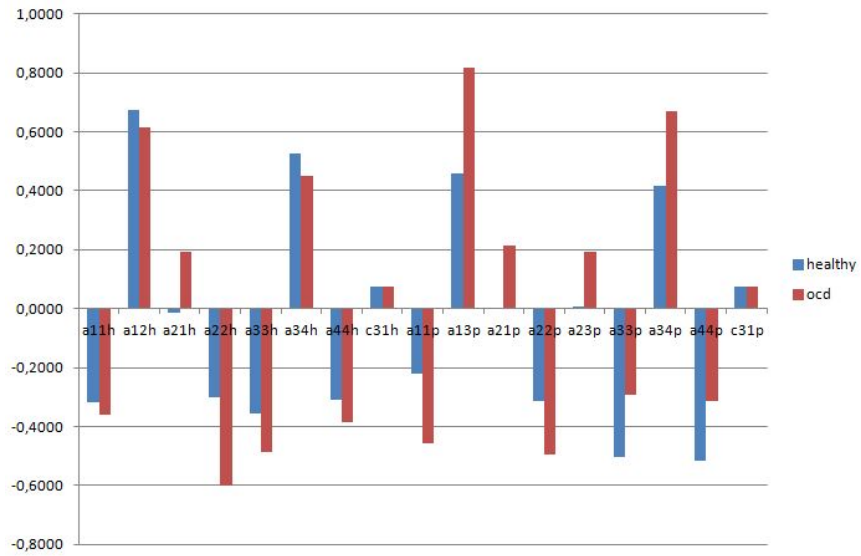
Figure B.17: Connectivity parameters of Subject 11 for best models H181 and P188
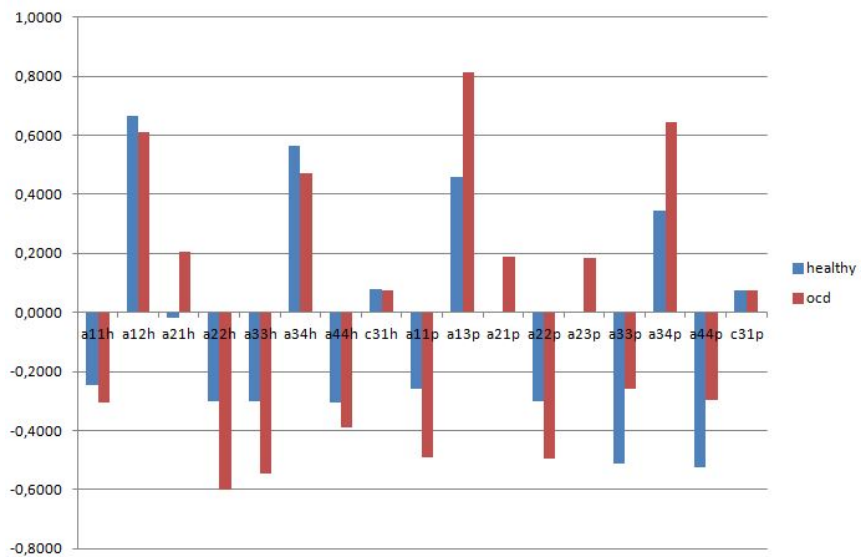
Figure B.18: Connectivity parameters of Subject 12 for best models H181 and P188

APPENDIX C

COSINE SIMILARITY

There are many methods to measure the similarity between vectors and cosine similarity method is one of them. Cosine similarity just measures the cosine of the angle between two vectors. Cosine similarity between two $d-$dimensional vector x, y is defined as in Equation C.1.

$$cos(x, y) = \frac{x.y}{\|x\|\|y\|} = \frac{\sum_{i=1}^{d} x_i y_i}{\sqrt{\sum_{i=1}^{d} x_i^2} \sqrt{\sum_{i=1}^{d} y_i^2}} \tag{C.1}$$

Cosine similarity can be used as feature extraction method and decision is made by comparison of similarities as in [13]. It measures the distance between each sample and the mean cluster of the other samples. This approach calculates the cosine value of the angle between the two vectors formed in chapter 4 Feature Extraction section for each subject and the means of healthy and patient subjects. LOO-CV algorithm is applied. Cosine similarity can be defined as:

If test subject k is healthy subject:

$$f_1 = cos(S(k), meanS_{H-k})$$
$$f_2 = cos(S(k), meanS_P) \tag{C.2}$$

where f_1 and f_2 cosine of the angle between test subject (k^{th} subject) and mean vector of the remaining healthy subjects (training healthy subjects) and training OCD subjects. S(k) is the feature vector of kth subject, S_{H-k} healthy subject feature vectors without k^{th} subject and S_P OCD subject feature vectors.

Otherwise, when test subject k is OCD subject:

$$f_1 = cos(S(k), meanS_H)$$
$$f_2 = cos(S(k), meanS_{P-k})$$

(C.3)

where S_{P-k} OCD subject feature vectors without k^{th} subject

Decision is made by comparison of similarities, therefore the class of the test sample k can be decided simply by comparison of f_1 and f_2 such that:

$$if f_1 > f_2$$
$$k\epsilon H$$
$$Otherwise$$
$$k\epsilon P$$

(C.4)

By using feature vectors obtained in chapter 4 and applying LOO-CV algorithm, the cosine similarity is obtained. For each subject, the cosine of angle is measured for the model 188 which is the best model for OCD and second model for healthy groups. The cosine of angle between mean values for both group is calculated as 0.8778. Subject vs mean values results are presented in Table C.1 as class represents the true class of each subject. Also, f_1 and f_2 values and decisions from these values are given. Performance is 1 if class and decision is matched and 0 otherwise. Total performance is calculated from the proportion of the sum of performances over subject number, 24.

From this similarity analysis, 79,16% accuracy is obtained. Therefore the performance of this analysis is lower than the SVM analysis.

Table C.1: Cosine Similarity Results

Test Subjects	Class	f1	f2	Decision	Performance
1	H	0,97	0,96	H	1
2	H	0,98	0,95	H	1
3	H	0,98	0,95	H	1
4	H	0,99	0,93	H	1
5	H	0,97	0,96	H	1
6	H	0,99	0,92	H	1
7	H	0,91	0,99	P	0
8	H	0,98	0,95	H	1
9	H	0,98	0,95	H	1
10	H	0,95	0,98	P	0
11	H	0,96	0,97	P	0
12	H	0,97	0,96	H	1
13	P	0,96	0,97	P	1
14	P	0,97	0,96	H	0
15	P	0,95	0,98	P	1
16	P	0,96	0,97	P	1
17	P	0,92	0,99	P	1
18	P	0,99	0,93	H	0
19	P	0,91	0,99	P	1
20	P	0,95	0,98	P	1
21	P	0,96	0,97	P	1
22	P	0,92	0,99	P	1
23	P	0,94	0,98	P	1
24	P	0,91	0,99	P	1
Total Performance (19/24)					79,16%